Radiochemistry Webinars
Nuclear Materials Analysis: Physical Methods of Characterization

In Cooperation with our University Partners

Meet the Presenter…

Dr. Jeff Terry

Dr. Jeff Terry is a professor of physics at the Illinois Institute of Technology, where his main research focus is on energy systems. His group works to develop new ways of dealing with radioactive waste, understand radiation damage mechanisms in materials, and synthesize novel materials for energy storage and conversion. He also simulates the economic costs of building new energy systems, including small modular nuclear reactors. Prior to joining the faculty at Illinois Tech, he was a staff scientist at Los Alamos National Laboratory (LANL). There, he worked on the Stockpile Stewardship and Management Program and the Waste Isolation Pilot Plant (WIPP) and was a member of the LANL team that sent the first waste shipment to WIPP. He is a former scientific director of the Advanced Test Reactor National Scientific User Facility.

Dr. Terry is very active in science communication. He writes a regular column for the Bulletin of the Atomic Scientists and is an editor for the journal Applied Surface Science.

Dr. Terry earned his doctorate in chemical physics from Stanford University in 1997 and his bachelor's degree in chemistry from the University of Chicago in 1990.

Contact Information: terryj@iit.edu

ILLINOIS INSTITUTE OF TECHNOLOGY

Physical Methods of Characterization of Advanced Nuclear Materials

Dr. Jeff Terry
Illinois Institute of Technology

National Analytical Management Program (NAMP)
U.S. Department of Energy Carlsbad Field Office
TRAINING AND EDUCATION SUBCOMMITTEE

Nuclear Materials Science

- PWR Sustainability
  - Average age of 439 operating nuclear reactors is 24 years
  - Average age of 119 shutdown reactors 22 years
  - The Bulletin of the Atomic Scientists 2008 Status Report
- Push Lifetime To 40, 60, 90 Years
  - Aging
  - Stress
  - Corrosion
  - Fatigue
  - Irradiation effects

Nuclear Materials Science

- Beyond design basis
  - High temperature
  - Fuel cladding reactions
  - Hydrogen generation

Nuclear Materials Science

- Gen IV
  - Reactor design
  - Materials issues
  - Corrosion
  - Neutronics
  - High temperature
- Fuel
  - Corrosion
  - Pellet cladding interaction
  - Fission gas release and swelling
  - Hydrogen induced embrittlement of cladding alloys

Nuclear Materials Science

- Nuclear Waste
  - Fate
  - Transport
  - Geochemistry
  - Biochemistry
  - Repository Science
- Fundamental Science
  - 5f Electron Behavior
  - Highly correlated electrons
  - 5f Chemistry

Techniques

- Electronic Structure
  - Photoelectron Spectroscopy
  - X-ray Absorption Near Edge Spectroscopy
  - Tunneling Spectroscopy
  - X-ray Emission Spectroscopy
- Geometric Structure
  - Extended X-ray Absorption Fine Structure
  - X-ray Scattering
  - Electron Microscopy
  - Scanning Probe Microscopy
  - Atom Probe
- Physical Structure
  - Tomography

Probes

- Scattering Probes

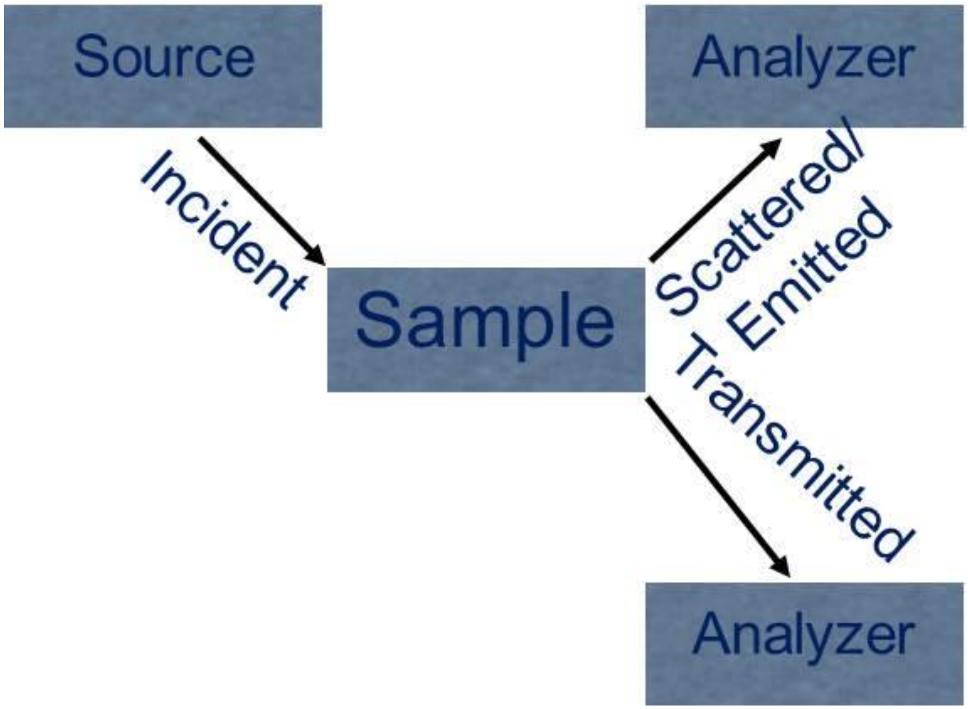

In	Out	Name
photon	0	Absorption
photon	photon	Fluorescence, Raman, Compton
photon	electron	Photoelectron Spectroscopy
photon	electron *electron	Auger
electron	electron *electron	Auger
electron	photon	X-ray Emission
electron	electron	Energy Loss
electron	electron	Microscopy
ion	ion	Secondary Ion Mass Spectroscopy

Electronic Structure

- Chemical Environment - Energy Position
- Physical Environment - Broadening

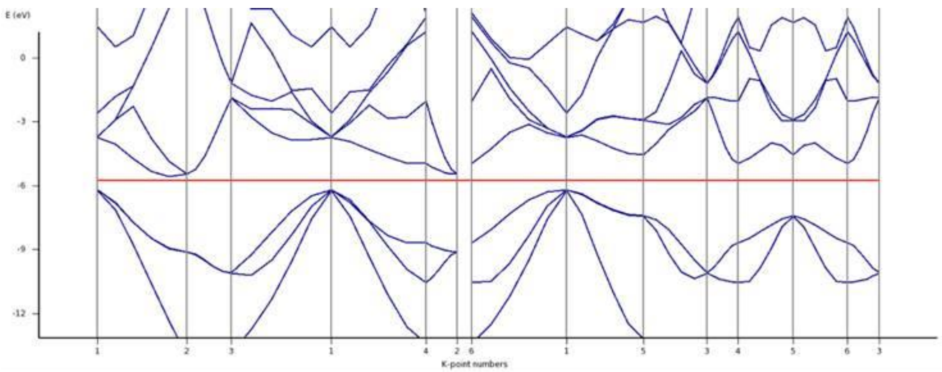

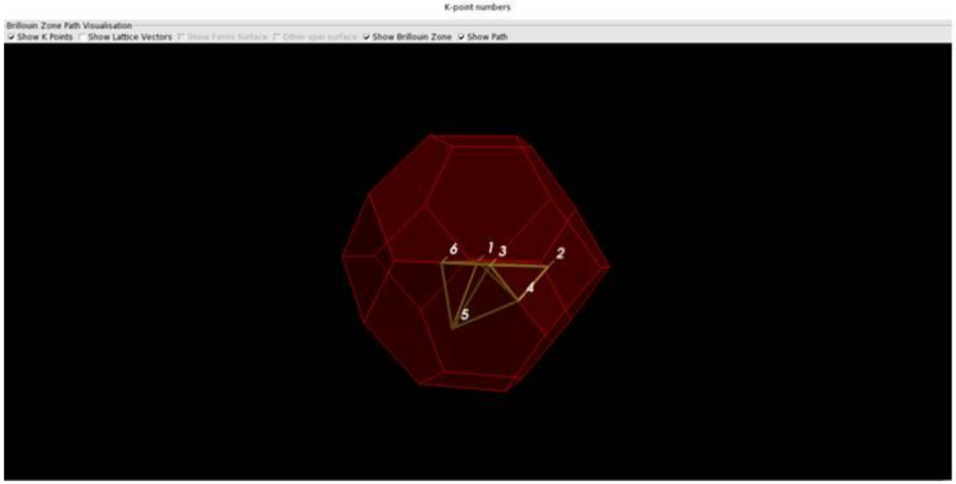

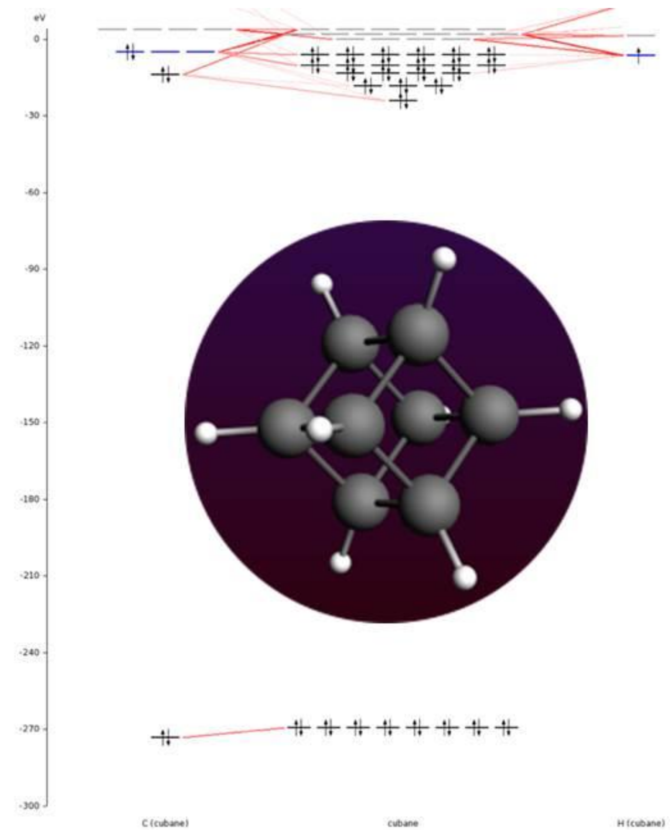

Photoelectron Spectroscopy

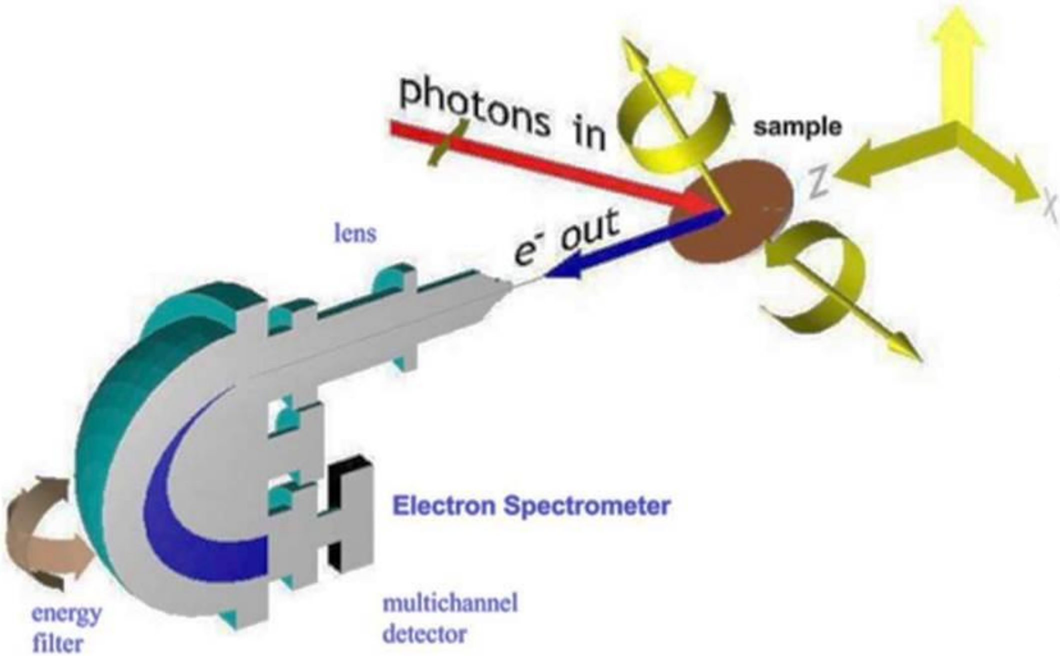

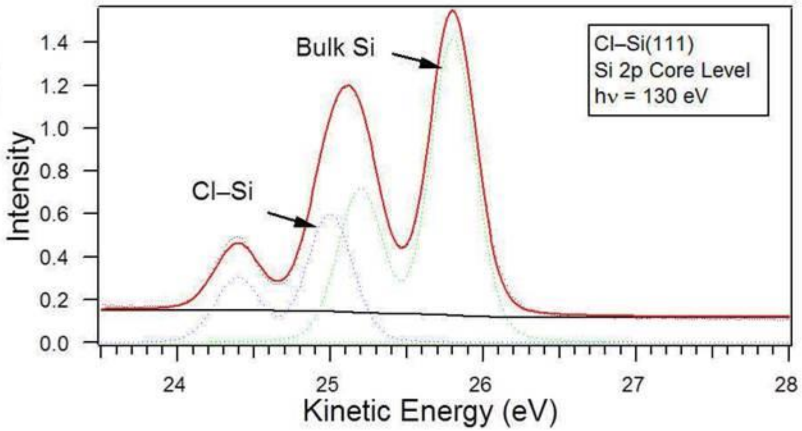

From Rotenberg: www-bl7.lbl.gov/BL7/who/eli/SRSchoolER.pd

Resonant Photoemission of Pu

- 5f Electron systems are different

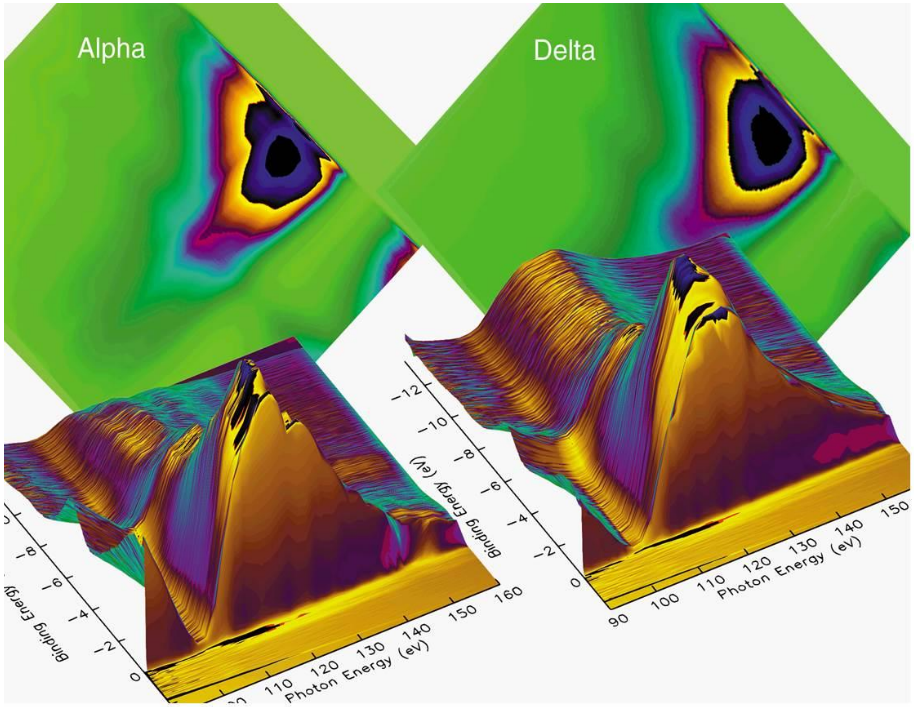

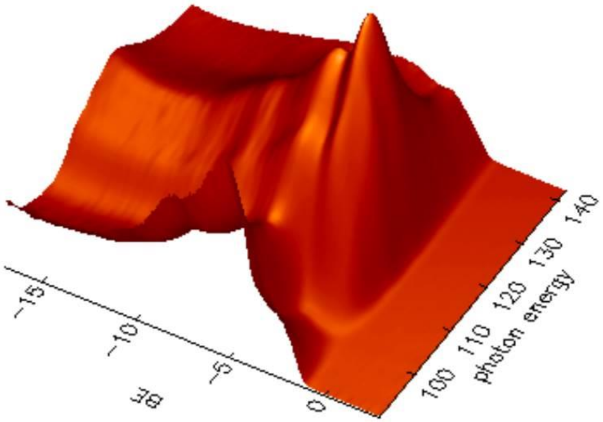

(Pu(VI)OH) pH 5.5

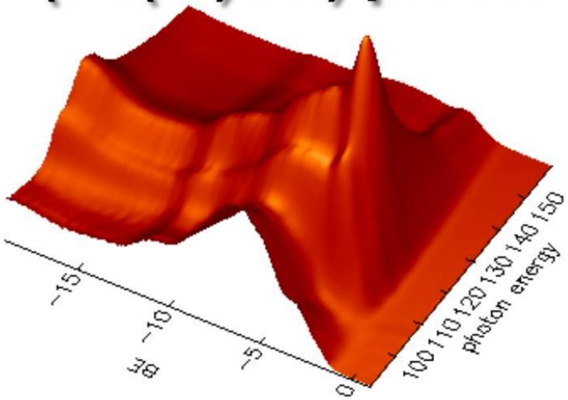

Pu(V) on SiO_2/Si

Terry, J, et al., Surface Science 499, L141 (2002)
Tobin, J. G, et al., Physical Review B 68, 155109 (2003)

Resonant Photoemission of Pu

- Fano profile
- FCC Pu suggests more atomic-like character

$q \sim \langle 5d^{10}5f^{5}|r|5d^{9}5f^{6}\rangle / \langle 5d^{10}5f^{5}|r|5d^{10}5f^{4} + e^{-}\rangle$

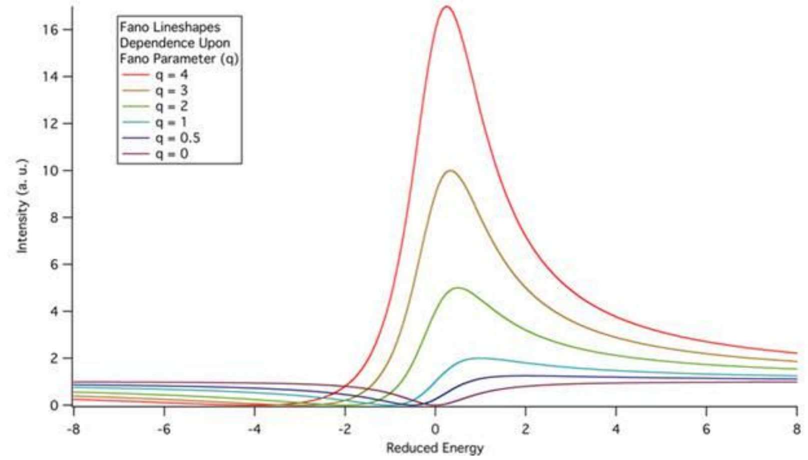

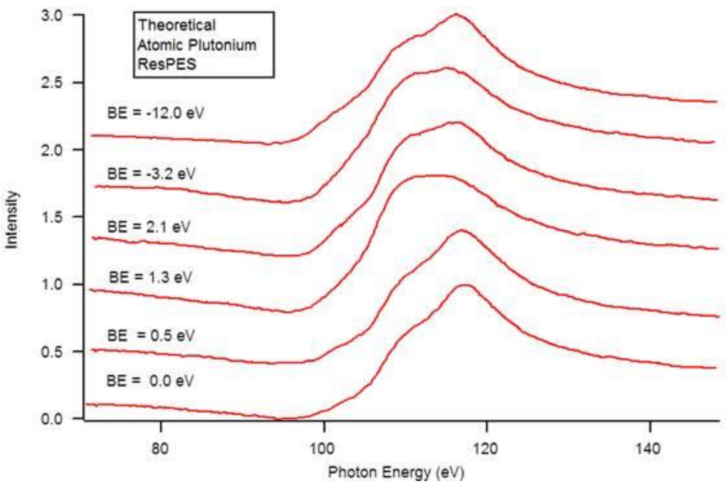

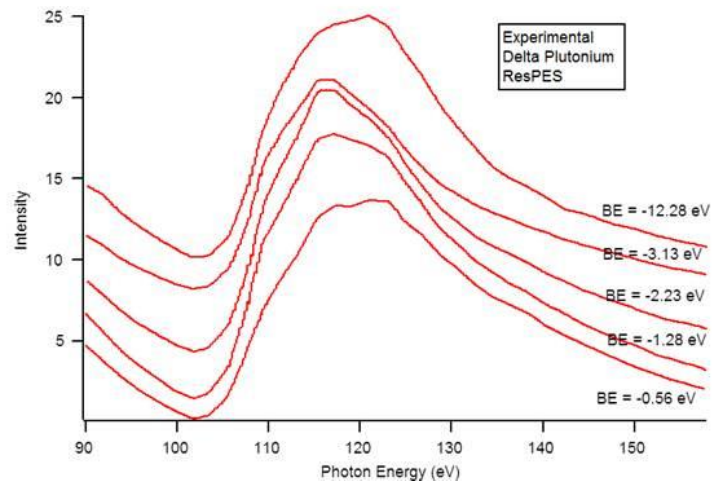

Terry, J, et al., Surface Science 499, L141 (2002)
Tobin, J. G, et al., Physical Review B 68, 155109 (2003)

Photoemission Of Disordered Alloys

- High resolution core level spectroscopy allows one to measure disorder broadening
- Can now calculate by calculating the core level shift for every atom

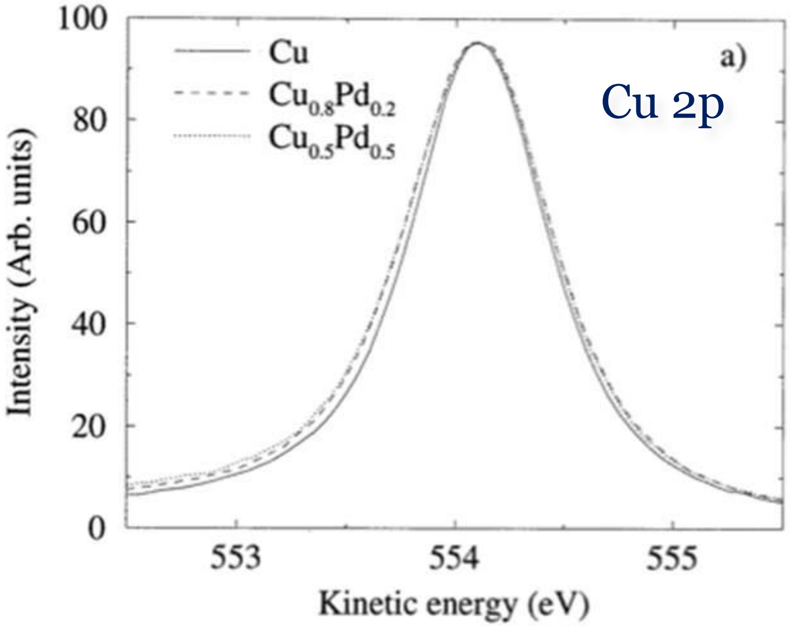

Cole, et al., J. Phys.: Condens. Matter 10 (1998) 5679–5695.

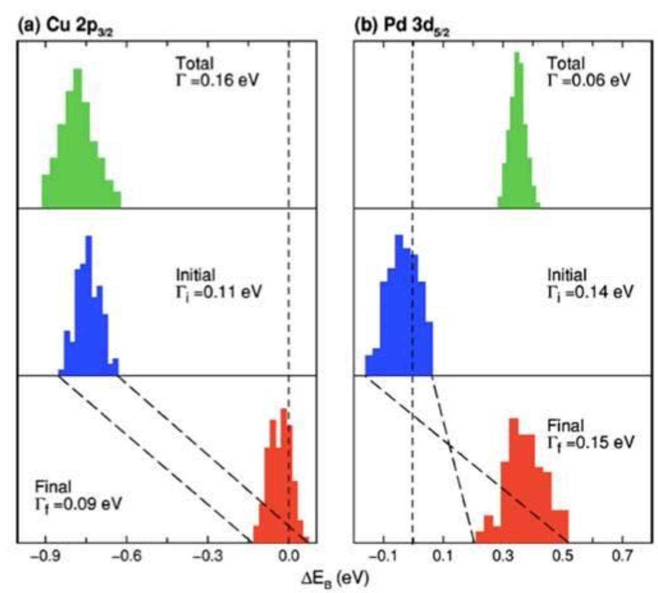

Martin, et al, PHYSICAL REVIEW B 72, 054210 (2005)
W. Olovsson et al. / Journal of Electron Spectroscopy and Related Phenomena 178–179 (2010) 88–99

X-ray Absorption

- Photon In
- Electron Excite
- Electron Scatters
- Electron Interference

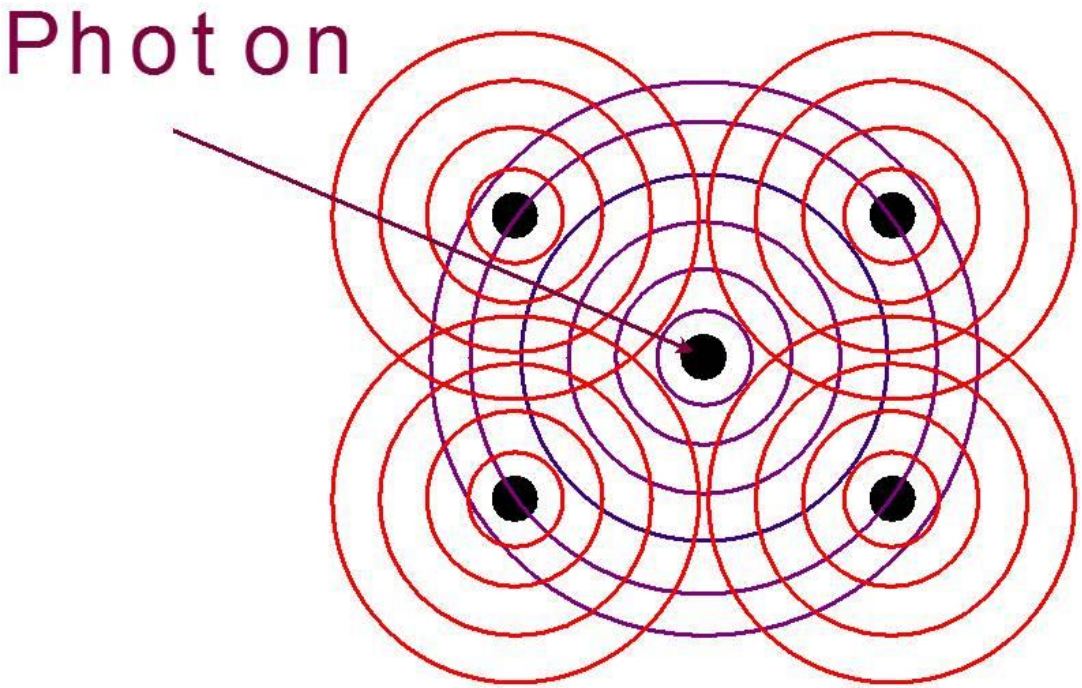

X-ray Absorption

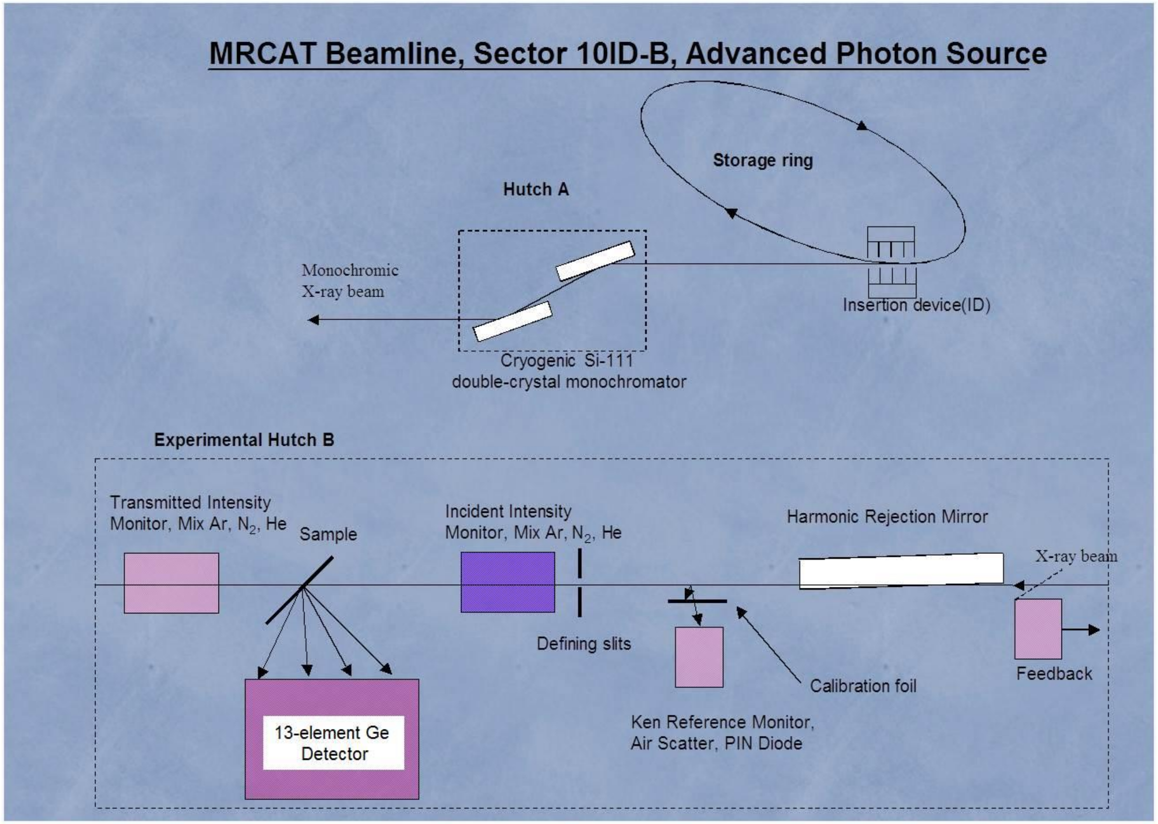

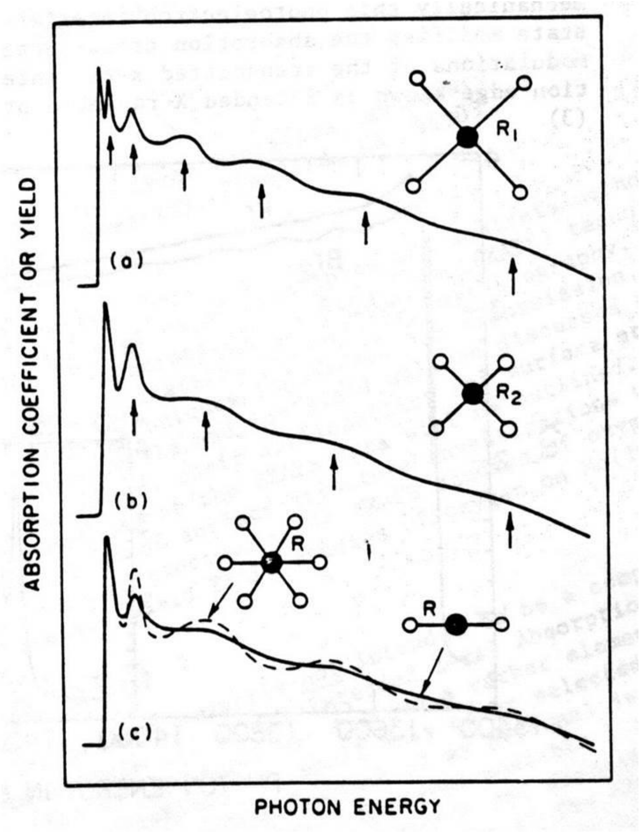

J. Stohr Nexafs Spectroscopy

XAS Analysis

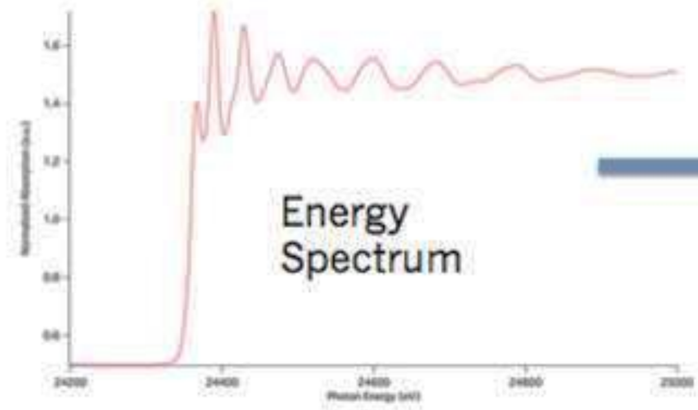

Convert to k-space and extract oscillations as a function of wavenumber

$$\mathbf{k} = \sqrt{\frac{\mathbf{2m(E - E_0)}}{\hbar^2}}$$

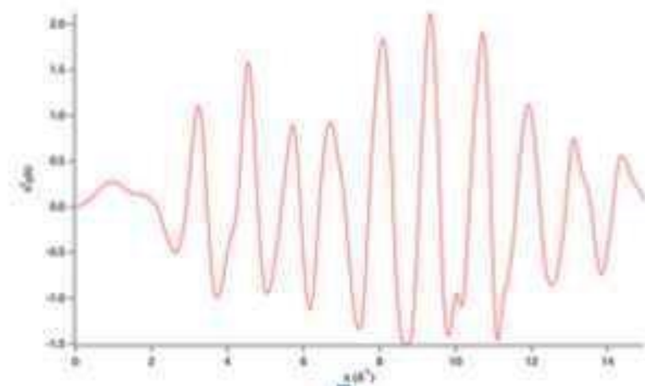

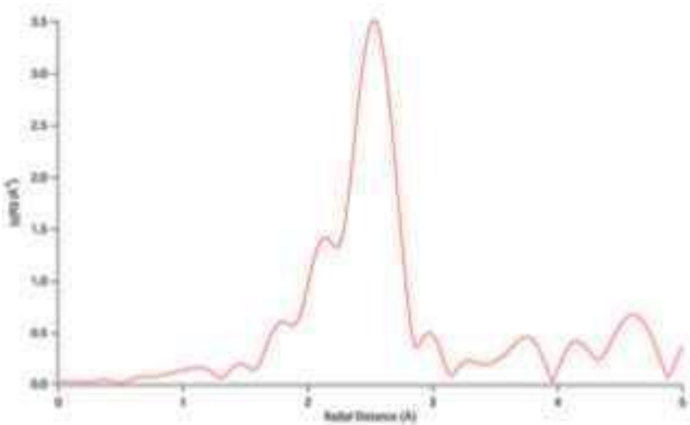

Fourier transform into R-space

Irradiated Zircaloy-2

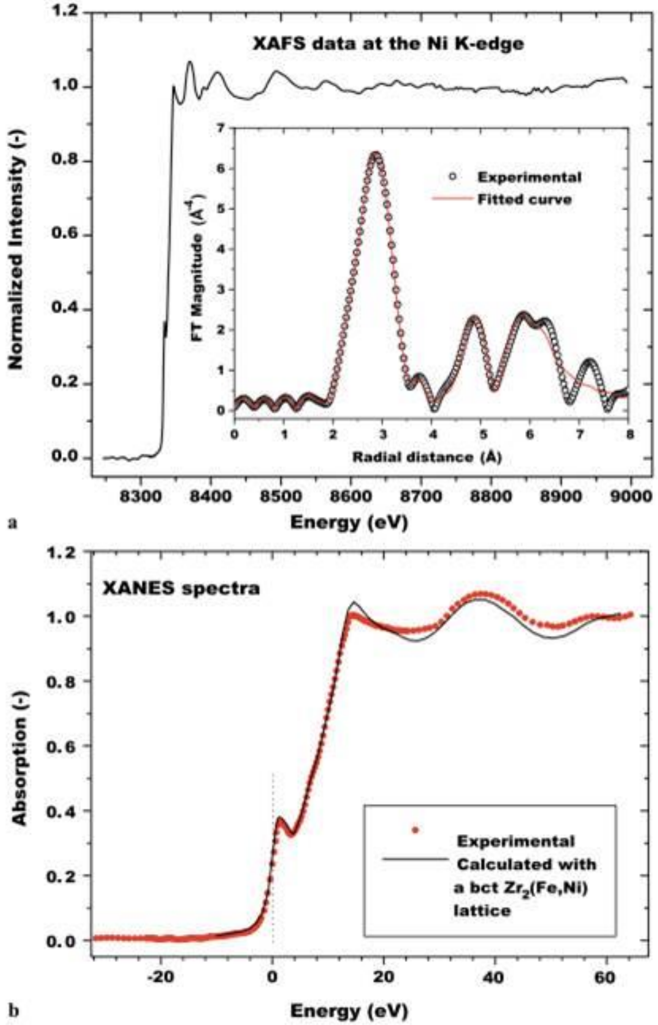

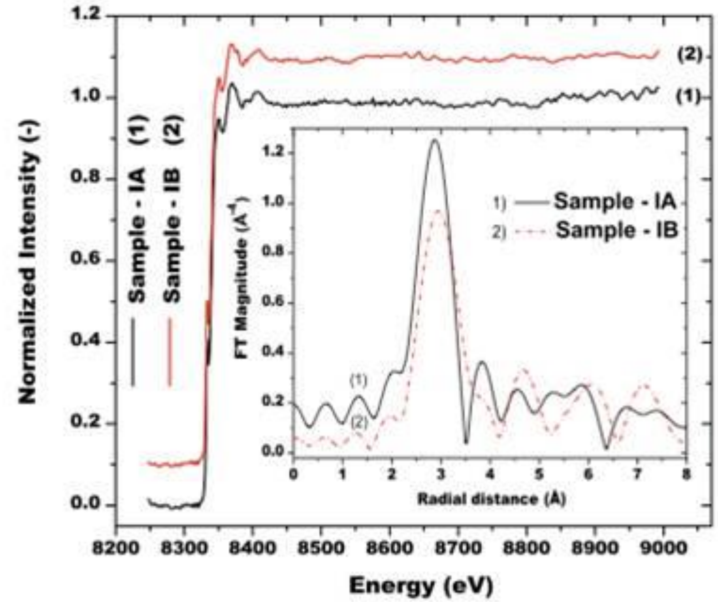

1A - 5.9 x 10^{21} n/cm^2

1B - 14.2 x 10^{21} n/cm^2

- $Zr_2Fe_{0.6}Ni_{0.4}$
- Dissolution and disorder of secondary phase

Kuri, et al., Appl Phys A (2010) 98: 625–633

ZrC as Cladding

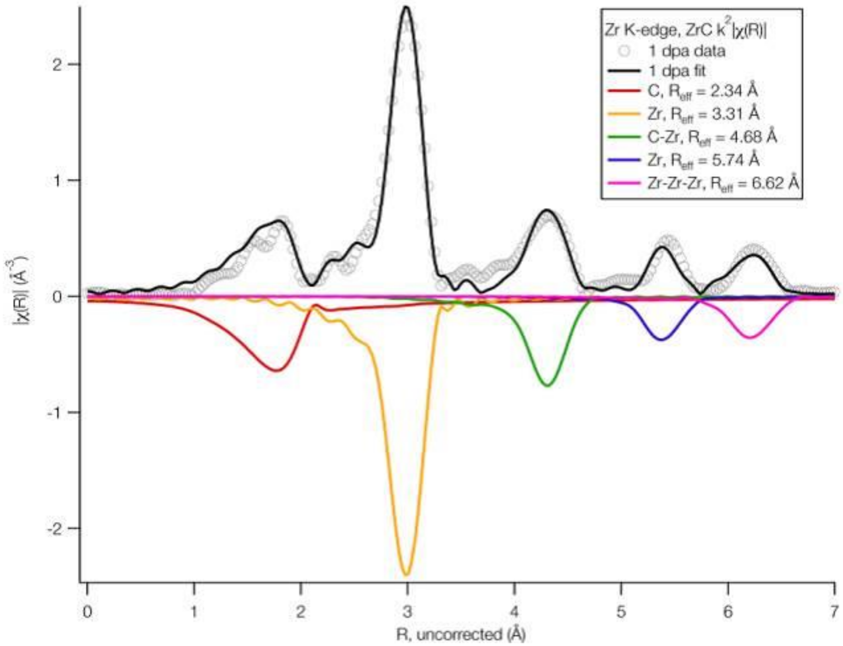

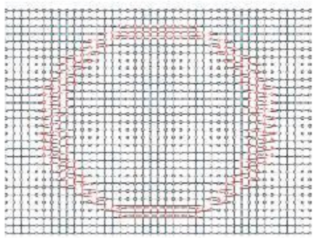

Olive, et al., Journal of Nuclear Materials 475, 123 (2016)

Fitting results for the simultaneous fit of the 0 and 1 dpa ZrC data. A single value of E_0 was used for all paths, the best fit was −1.12 ± 0.62 eV. Uncertainties determined by inversion of the covariance matrix.

Path[a]	$R_{PerfectCrystal}$ (Å)	$R_{Measured}$ (Å)	σ^2 (Å^2)	N, 0 dpa	N, 1 dpa	% Amplitude Difference
$Zr_0 \rightarrow C_1 \rightarrow Zr_0$	2.34	2.32 ± 0.02	0.008 ± 0.002	7.7 ± 2.6	6.6 ± 1.7	−14%
$Zr_0 \rightarrow Zr_1 \rightarrow Zr_0$	3.31	3.32 ± 0.02	0.004 ± 0.001	12.9 ± 3.5	9.3 ± 0.5	−28%
$Zr_0 \rightarrow C_1 \rightarrow Zr_2 \rightarrow Zr_0$	4.68	4.69 ± 0.02	0.005 ± 0.001	12.0 ± 2.0	7.8 ± 1.2	−35%
$Zr_0 \rightarrow Zr_3 \rightarrow Zr_0$	5.74	5.75 ± 0.02	0.003 ± 0.001	13.0 ± 3.5	6.0 ± 1.7	−53%
$Zr_0 \rightarrow Zr_1 \rightarrow Zr_4 \rightarrow Zr_1 \rightarrow Zr_0$	6.62	6.60 ± 0.02	0.005 ± 0.001	6.6 ± 1.8	2.8 ± 0.8	−57%

[a] The subscript represents *n*th coordination shell of a particular type of atom, 0 indicating the core scatting atom.

ZrC

- Sphere 1.8 nm in diameter
- Model undefected regions as spherical

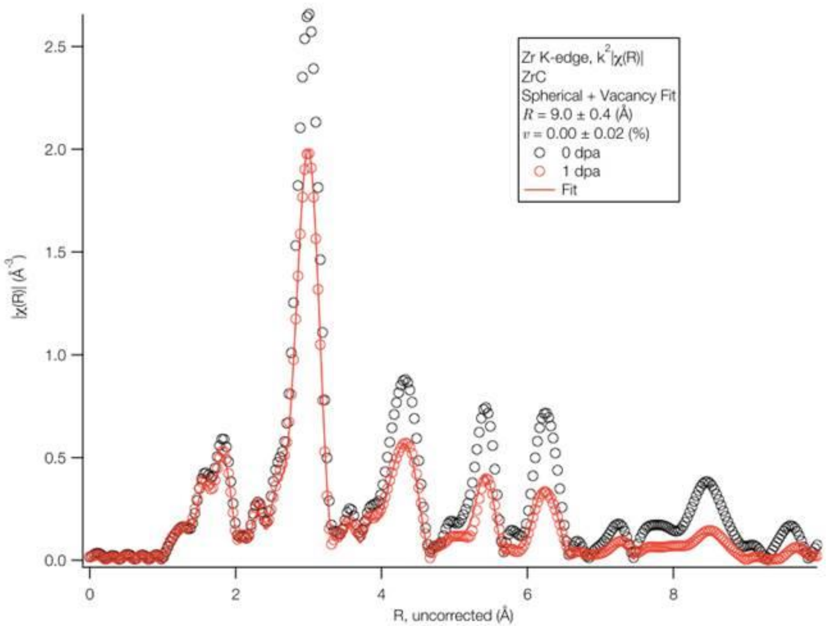

Fig. 8. Fitting results of the unirradiated ZrC sample to the 1 dpa sample, using the vacancy corrected spherical crystallite model.

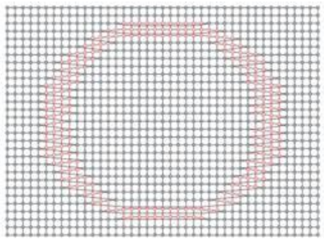

Olive, et al., Journal of Nuclear Materials 475, 123 (2016)

$$N_{\text{nano}} = \left[1 - \frac{3}{4}\left(\frac{r}{R}\right) + \frac{1}{16}\left(\frac{r}{R}\right)^3\right]\left(N_{\text{bulk}}(1 - v)\right)$$

X-ray Scattering

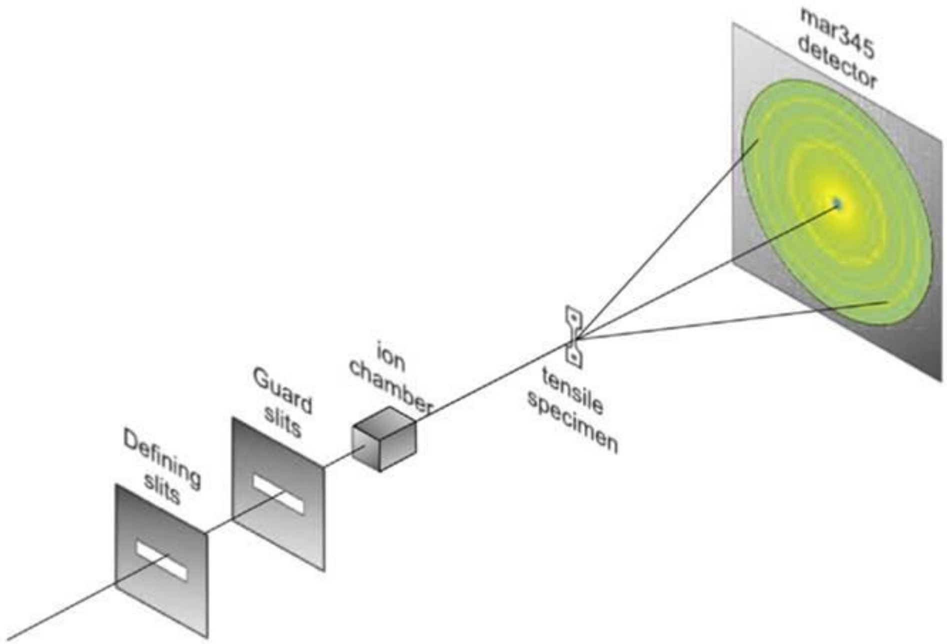

Liu, et al., Materials Science & Engineering A 651, 55 (2016)

Calculate lattice strains (elastic) from change in atomic spacing.

$$\varepsilon = \frac{d_{hkl} - d_0}{d_0}$$

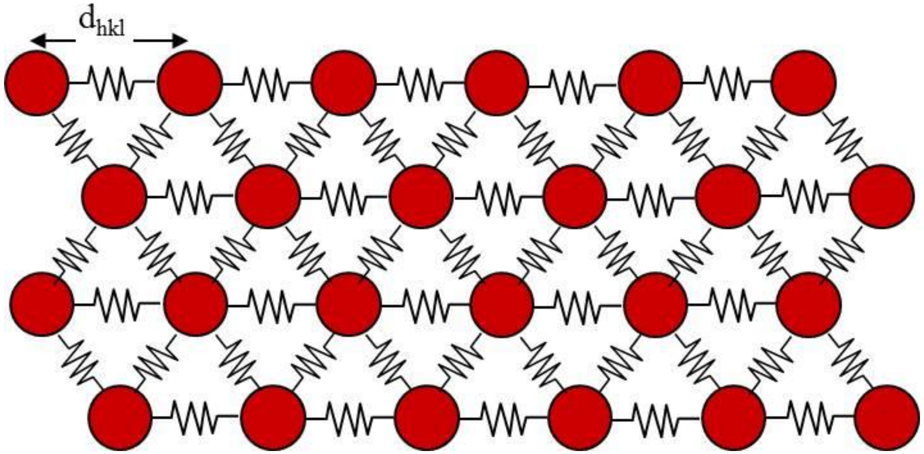

- Geometric structure
- Phase identification
- Size/Shape/Stress

Alloy 617: Intermediate Heat Exchanger (IHX) of VHTR

- $M_{23}C_6$ and M_6C
- Carbide phase analysis complicated by containment

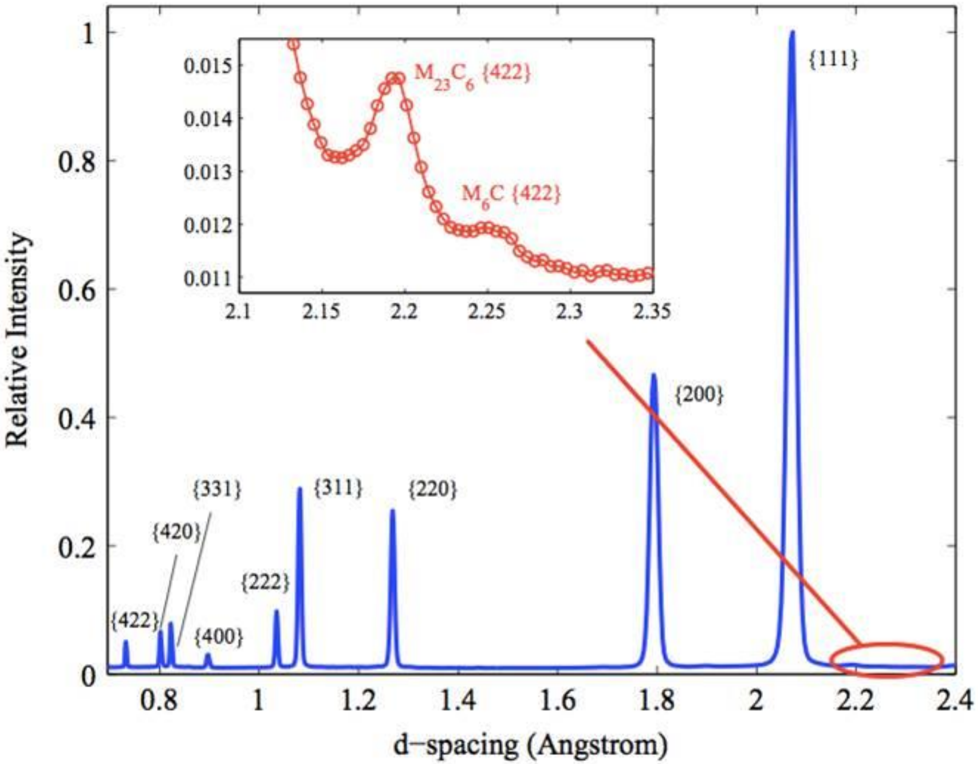

Fig. 3. The *d*-spacing plot of Alloy 617 at *t*=10,000 h showing {422} reflections from the $M_{23}C_6$ and M_6C phases. Major reflections from the face-centered cubic (FCC) matrix have also been indexed.

Liu, et al., Materials Science & Engineering A 651, 55 (2016)

Alloy 617: Intermediate Heat Exchanger (IHX) of VHTR

- Initial Linear Increase in $M_{23}C_6$ Lattice Strain

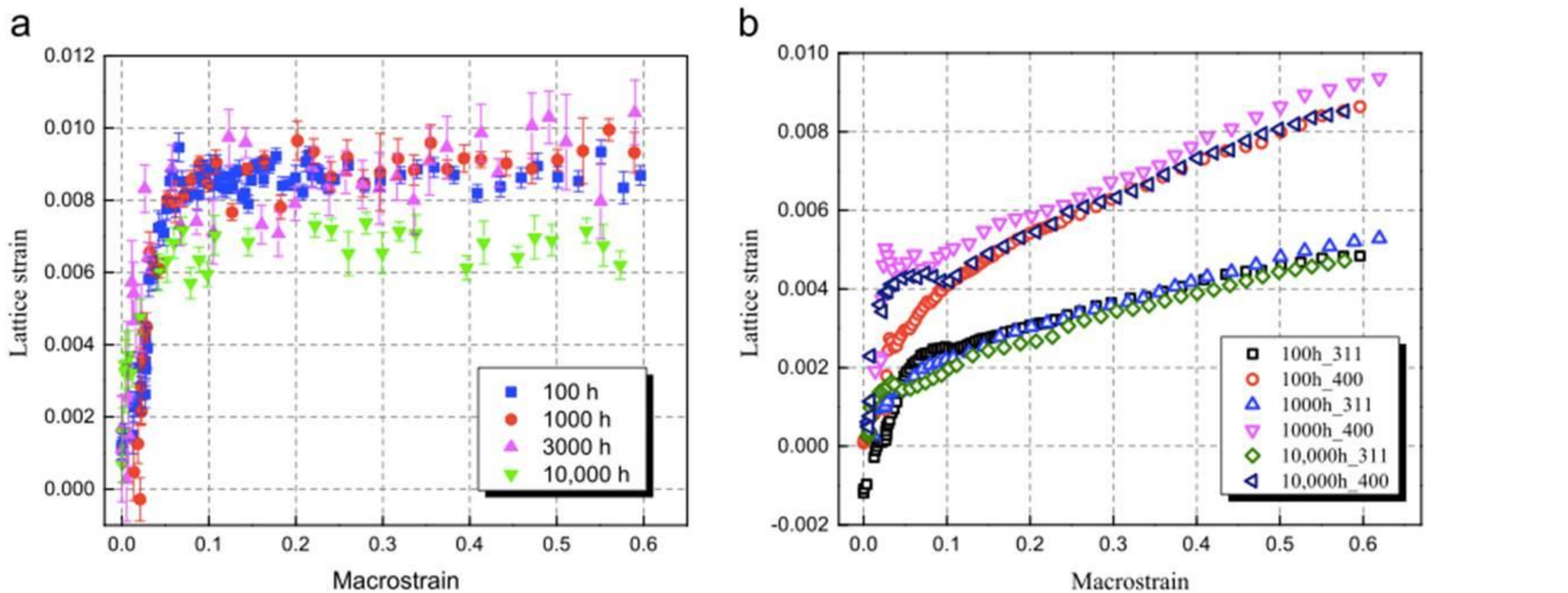

Fig. 6. Lattice strain evolution during the tensile loading: (a) the lattice strains of the $M_{23}C_6$ precipitate {422} reflection *vs* the macrostrain, and (b) the lattice strains of the metallic matrix {311} and {400} reflections *vs* the macrostrain, for Alloy 617 aged at 1000 °C to different times.

Liu, et al., Materials Science & Engineering A 651, 55 (2016)

Alloy 617: Intermediate Heat Exchanger (IHX) of VHTR

- Becomes constant as nucleation of microcracks or microvoids occur
- Leading to the fracture or decohesion of the particles

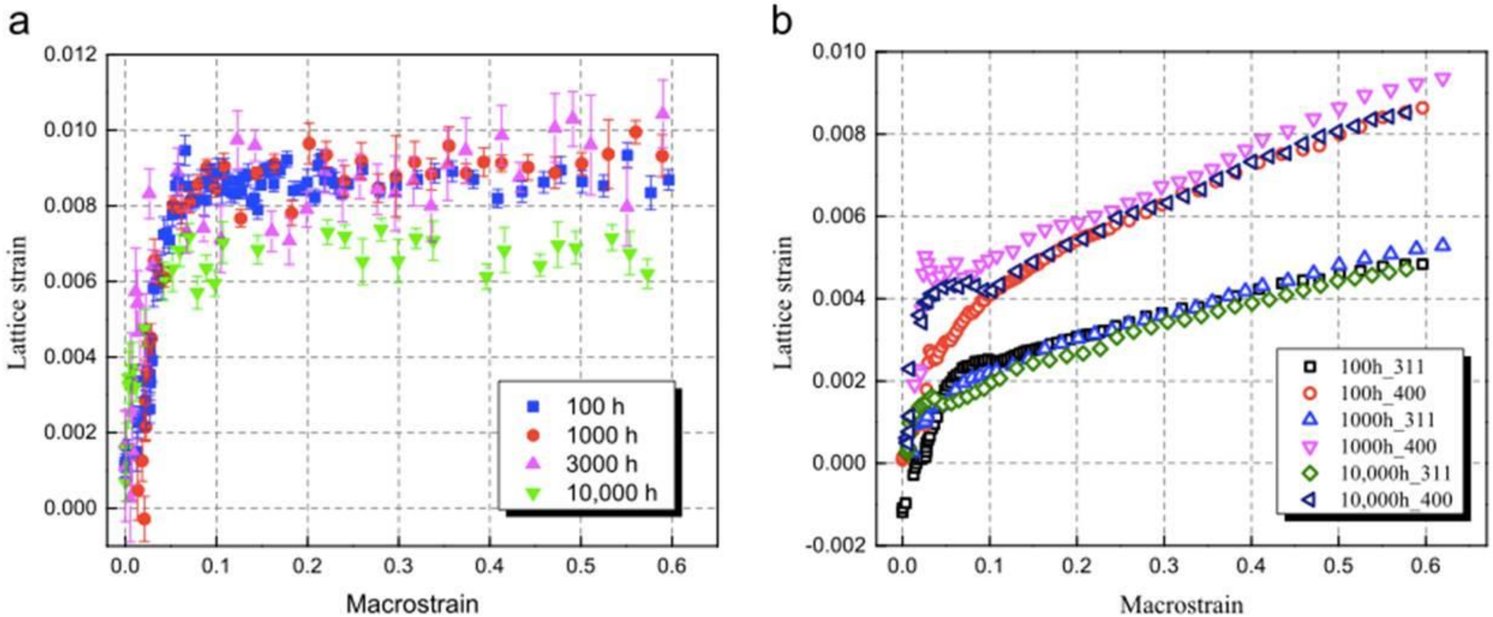

Fig. 6. Lattice strain evolution during the tensile loading: (a) the lattice strains of the $M_{23}C_6$ precipitate {422} reflection *vs* the macrostrain, and (b) the lattice strains of the metallic matrix {311} and {400} reflections *vs* the macrostrain, for Alloy 617 aged at 1000 °C to different times.

Liu, et al., Materials Science & Engineering A 651, 55 (2016)

U10Mo Fuel

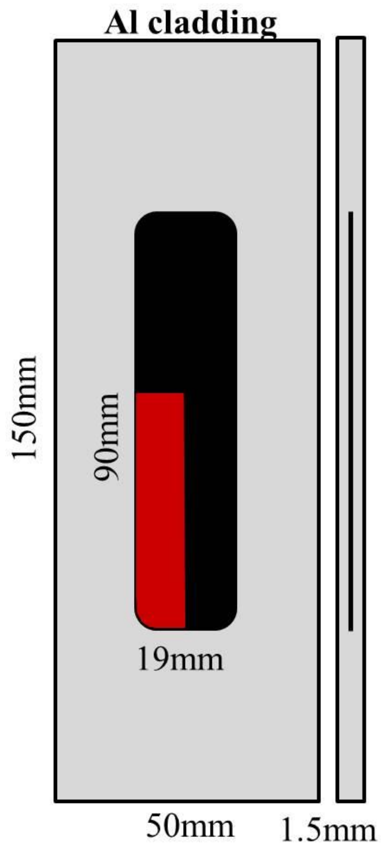

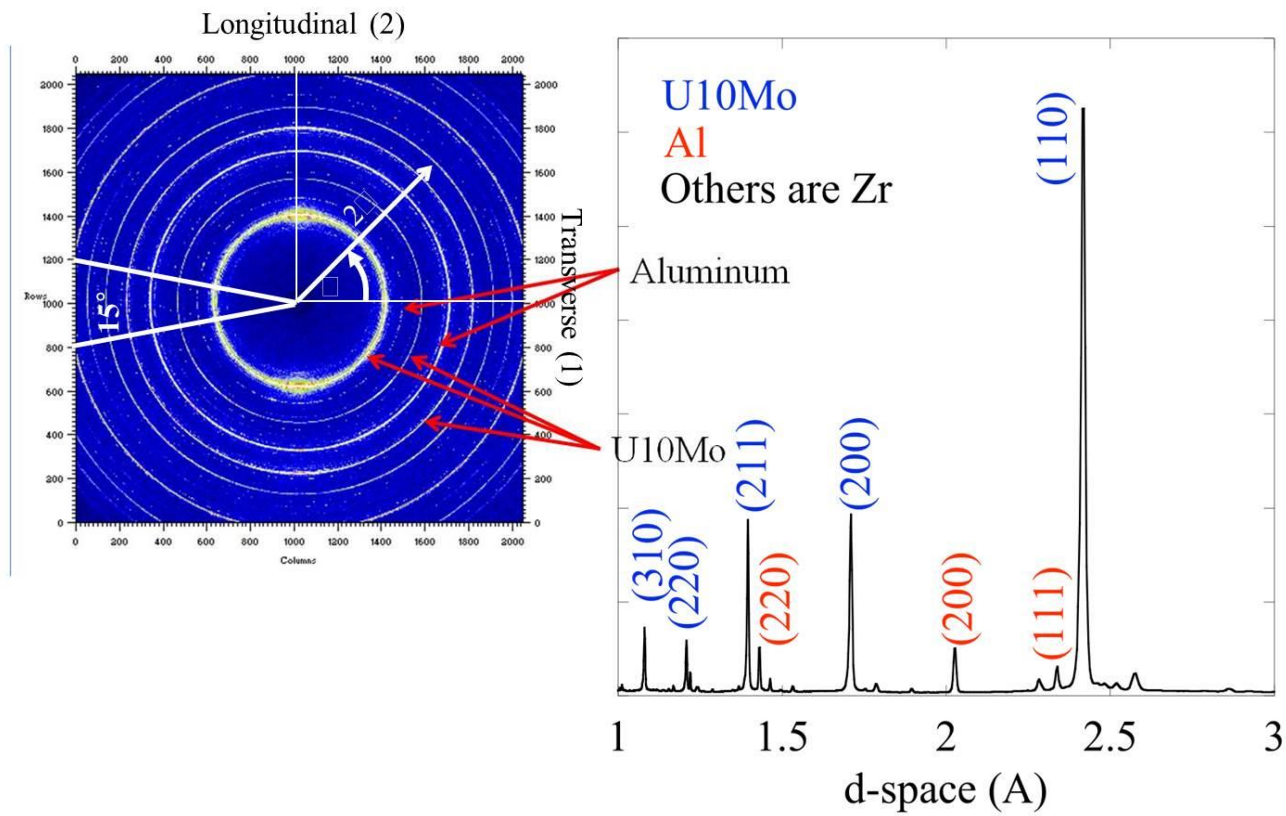

1.5 mm total thickness. 0.25mm thick U10Mo foil. Foil was cold rolled with Zr diffusion layer, then HIP bonded.

Okuniewski, et al., J. Nuc. Mater., submitted

U10Mo

- Map Full Strain Tensor

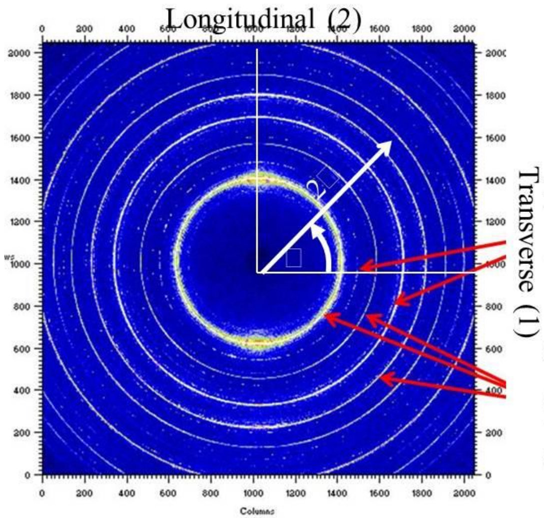

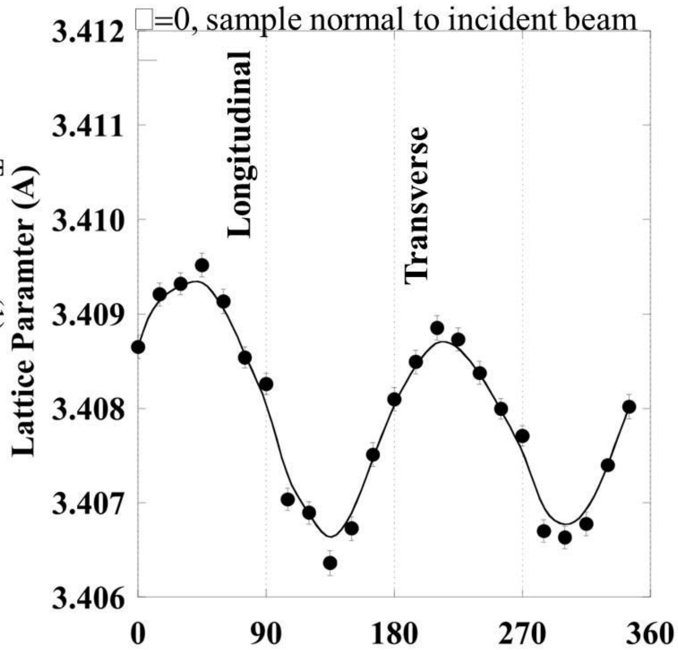

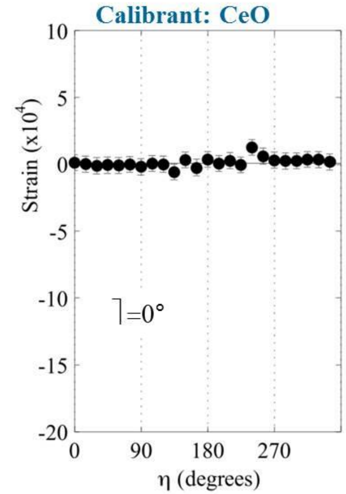

$$\varepsilon(\varphi,\psi) = \frac{d(\varphi,\psi) - d_0}{d_0}$$

6 fitting parameters, 72 measurements of *d* (□,□)

$$= \varepsilon_{11}\cos^2\phi\sin^2\psi + \varepsilon_{22}\sin^2\phi\sin^2\psi + \varepsilon_{33}\cos^2\psi + \varepsilon_{12}\sin 2\phi\sin^2\psi + \varepsilon_{23}\sin\phi\sin 2\psi + \varepsilon_{13}\cos\phi\sin 2\psi$$

Collect data at 3 sample angles, 0°, 45°, and 60°. Note, we cannot get a diffraction vector normal to the surface, i.e. □=90°

Okuniewski, et al., J. Nuc. Mater., submitted

U10Mo

- Rapid approach to zero stress at boundary suggest the material is not bonded on lateral interface

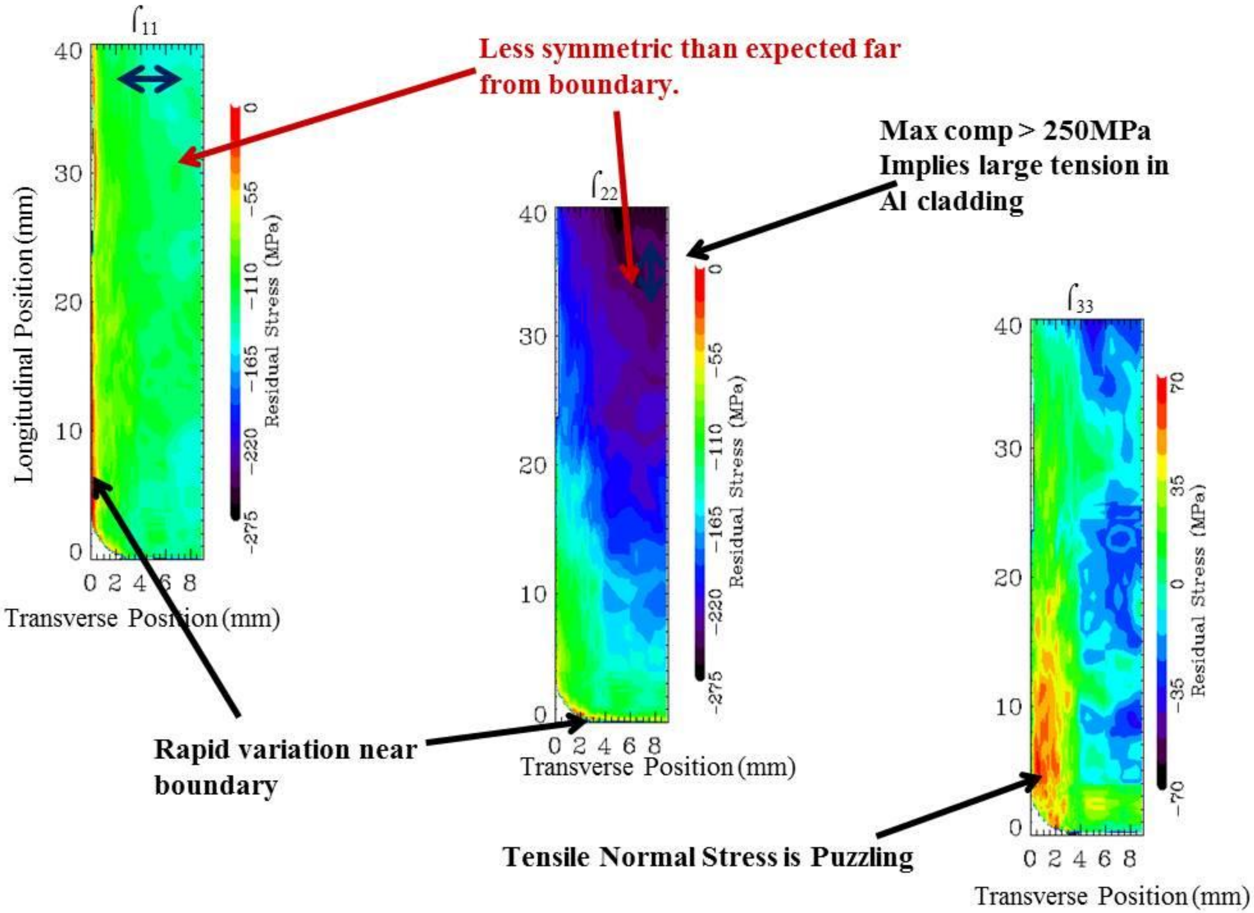

~5000 data points, 72 diffraction patterns per point = ~350K diffraction patterns

Okuniewski, et al., J. Nuc. Mater., submitted

Small Angle X-ray Scattering

- Sensitive To Shape and Distribution of Electrons

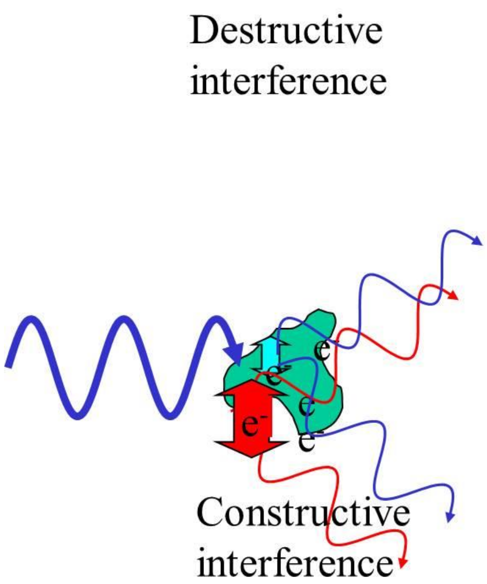

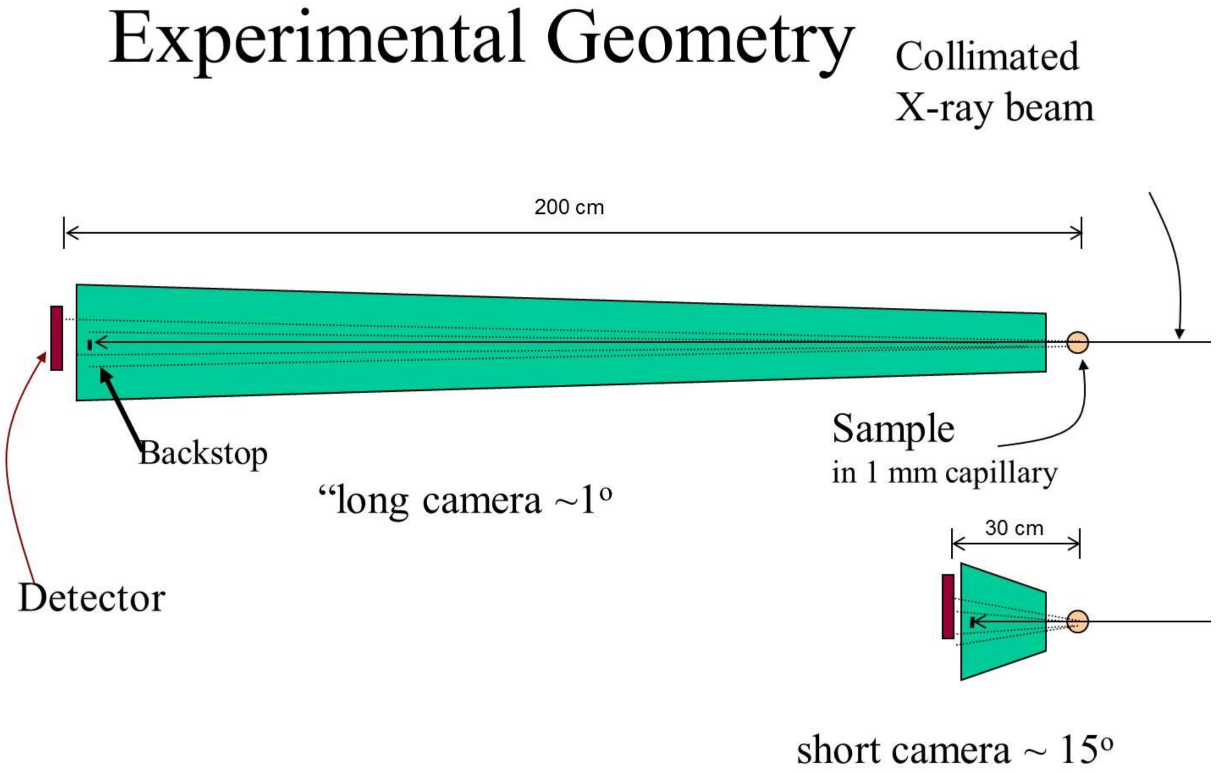

Irving unpublished

SAXS of ODS Steel

- $Y_2Ti_2O_7$ and Y_2TiO_5 nanoparticles at 960 C Diameter 2.6 nm

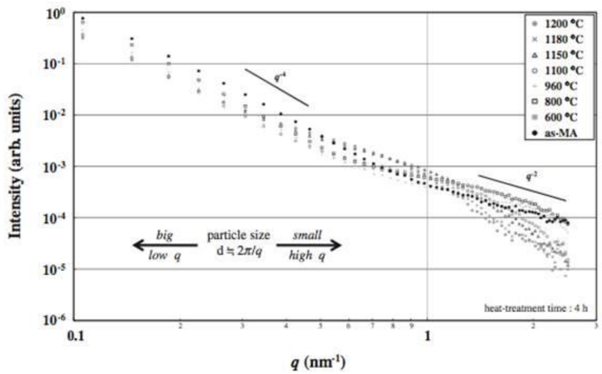

Fig. 3 SAXS profiles of as-MA powder and heat-treatment powders (600, 800, 960, 1100, 1150, 1180 and 1200°C for 4 h).

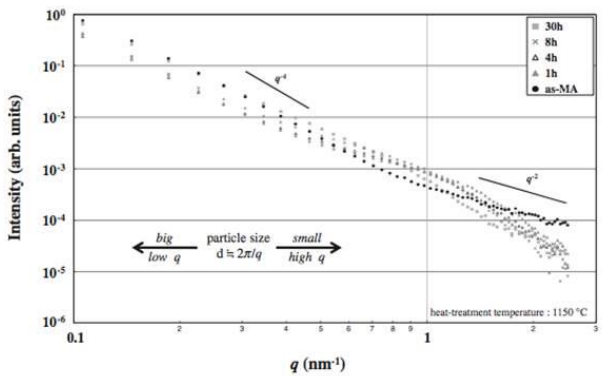

Fig. 4 SAXS profiles of as-MA powder and heat-treatment powders (1150°C for 1, 2, 4, 8, 15 and 30 h).

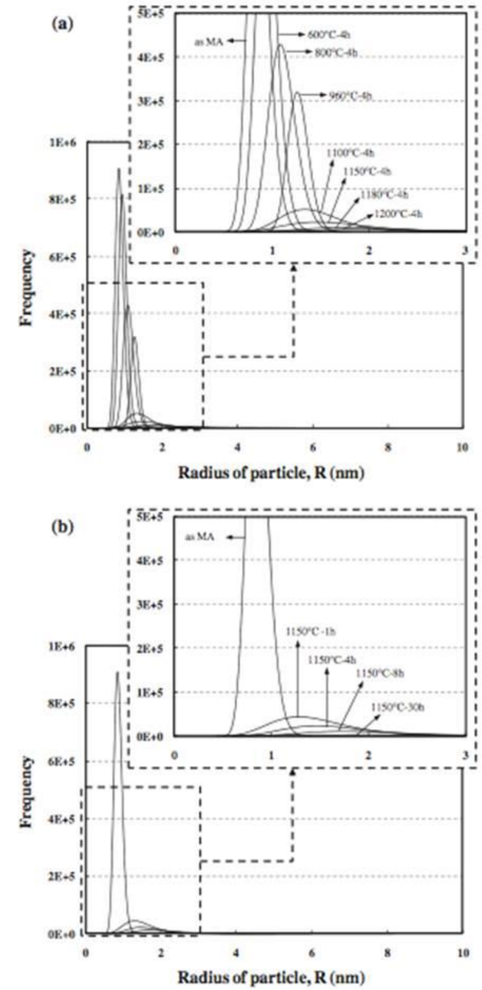

Fig. 5 Results of profile analysis for the distribution of particle size and frequency (a) effects of heat-treatment temperature; (b) effects of heat-treatment time.

Kim, et al., Materials Transactions, Vol. 50, No. 4 (2009) pp. 917 to 921

Tomography

- Microtomography

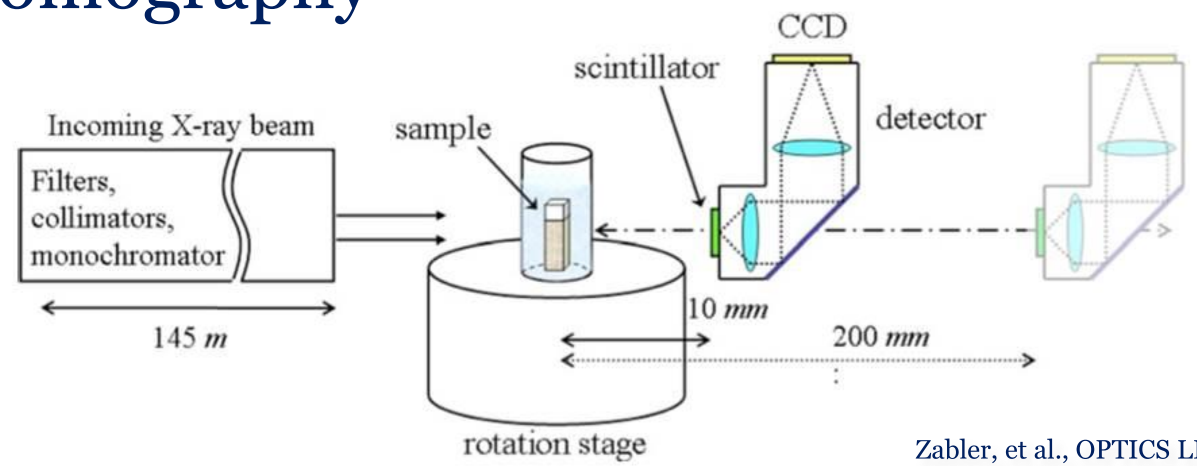

Zabler, et al., OPTICS LETTERS 32, 2987 (2007)

- Nanotomography

Schematic diagram of the Zernike phase contrast X-ray microscope

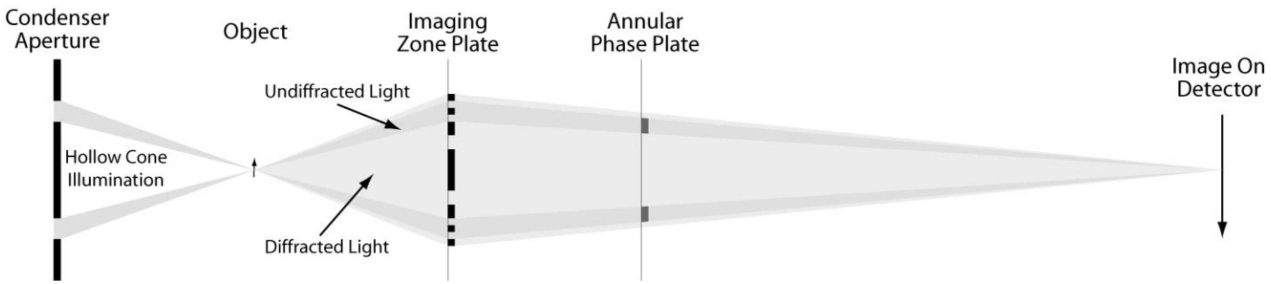

Pianetta unpublished

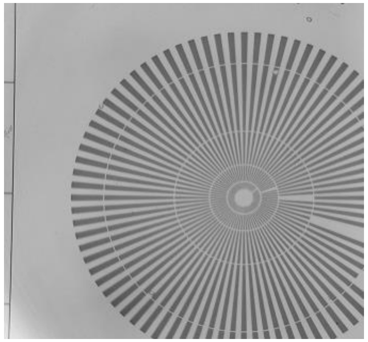

X-ray transmission image of the Siemens calibration standard with 30 nm minimum features. FOV: 30x30 microns²

Friction Weld Crack TiAl/Ti_6Al_4V

- 150 keV at 50 μm Resolution

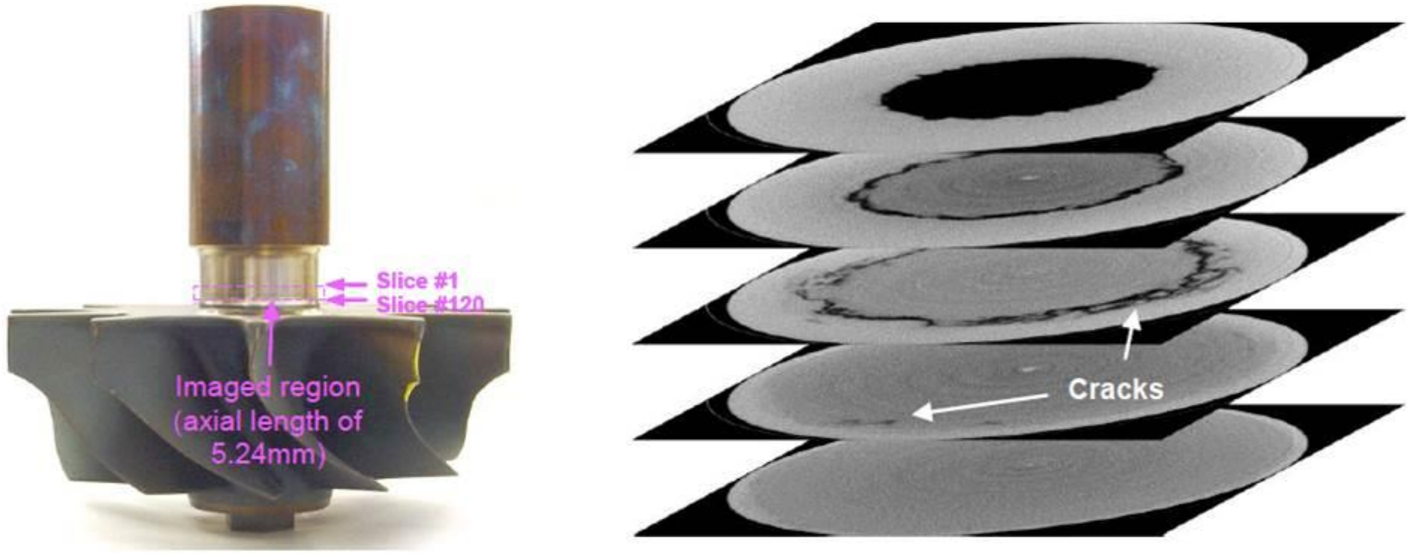

(a) (b)

FIGURE 6. (a) Welding sample #2 and (b) typical reconstructed X-ray CT slices around the welding interface (distance between two adjacent slices is 0.3 mm).

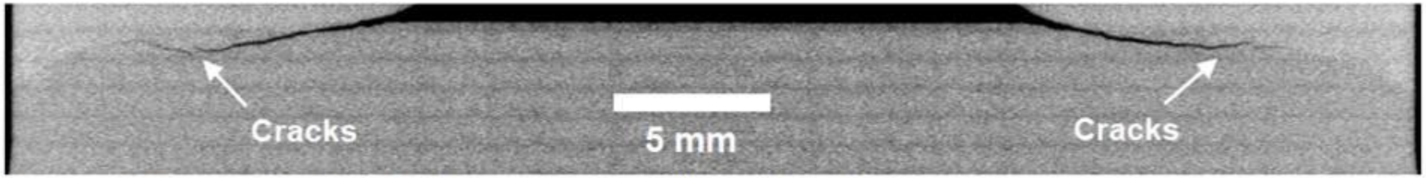

FIGURE 7. A re-sliced axial CT image of the weld sample #2 shown in Fig. 6a.

Sun, et al., AIP Conf. Proc. 1430, 1251-1258 (2012)

Tomography of Fuel Pin

- High Energy Tomography Of UO_2 Fuel In a Steel Clad Fuel Pin
  - White Beam Filtered To 251 KeV
  - Cadmium-Tungstate Scintillator - 5 µm Resolution

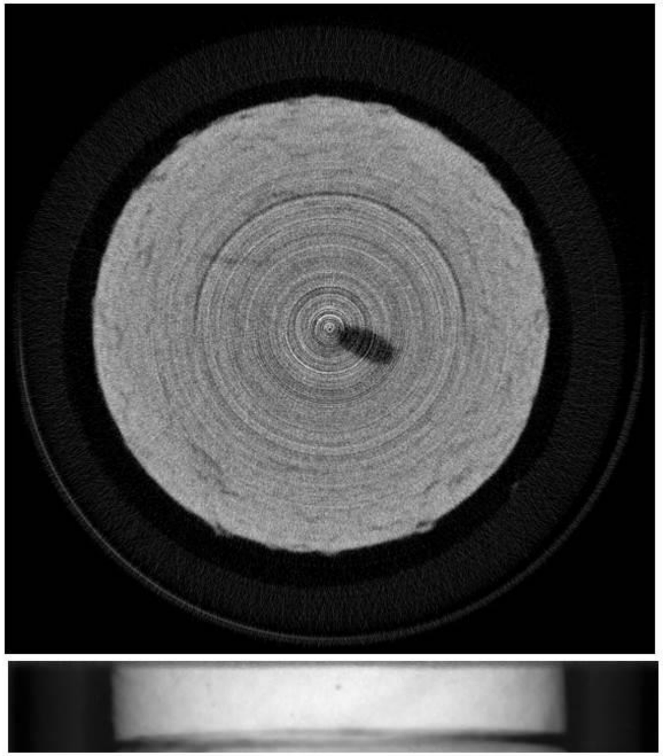

Bourke, et al., in preparation

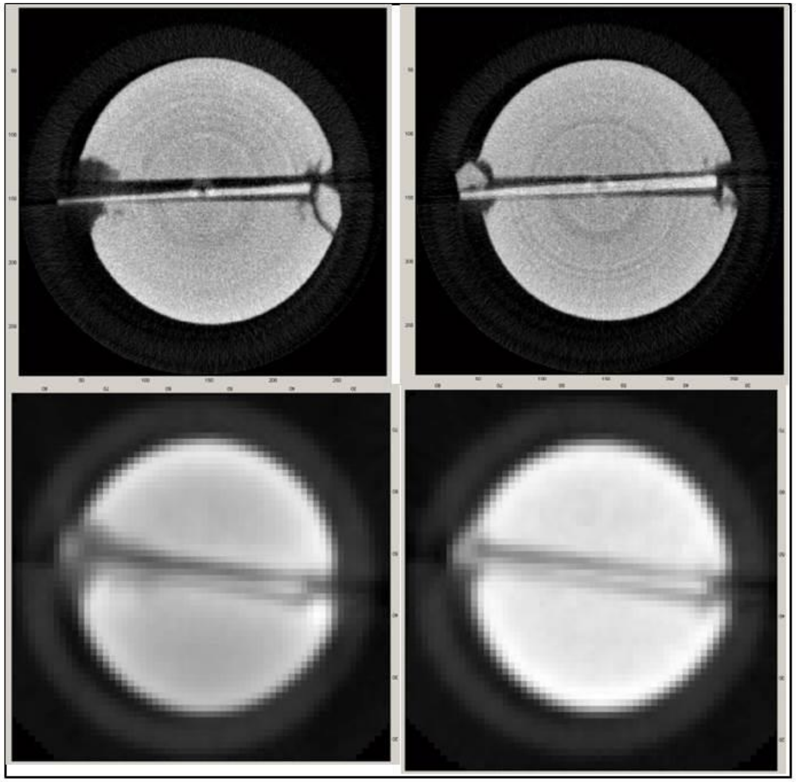

251 KeV Synchrotron Data (Top) vs LANL 450 KeV Brehmstralung Source

Mapping

- All the aforementioned techniques can be combined with mapping by using the spacial profile of the X-ray beam

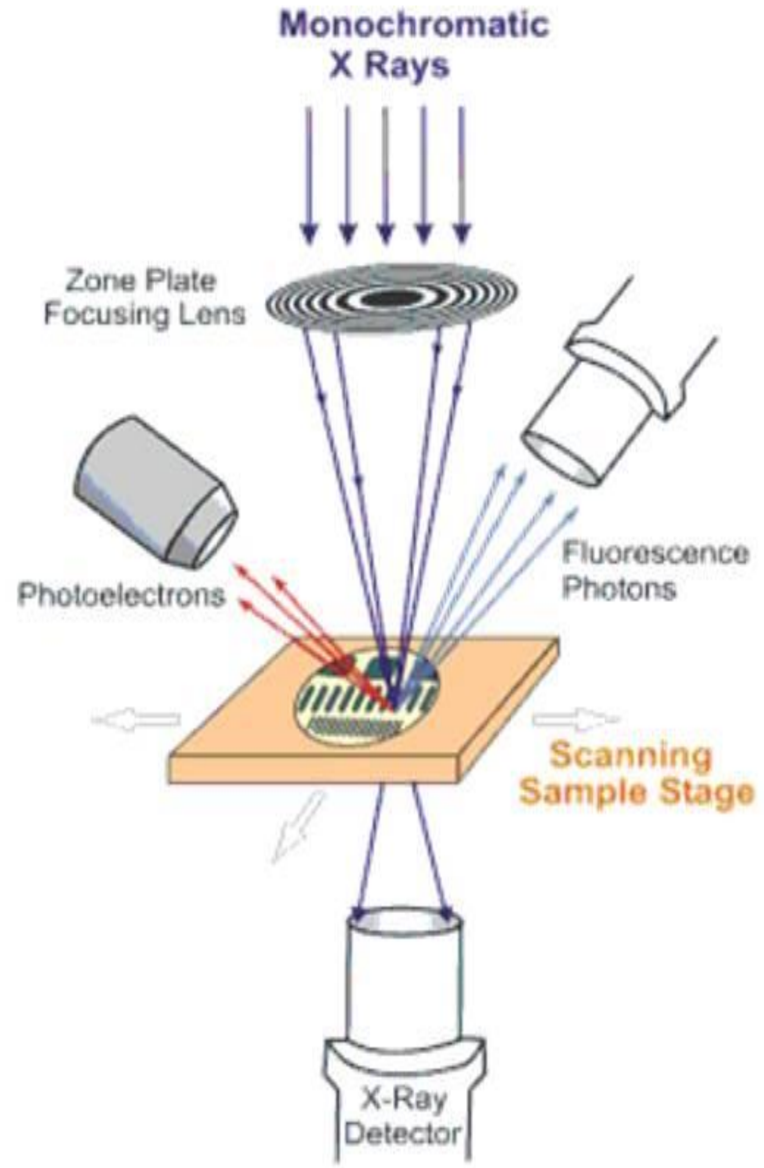

Pu(VI) Sorption on WIPP 1A Bacteria

- C K-edge Map
- 100 nm Resolution

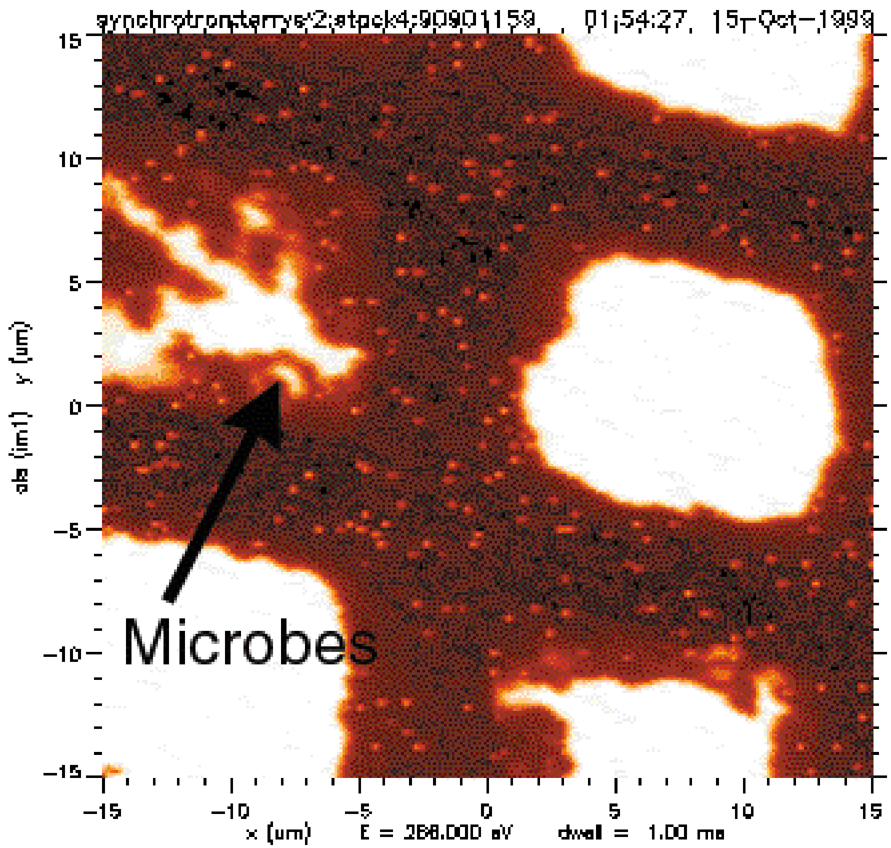

Strietelmeier, et al., LANL

Corrosion of Commercial Spent Fuel

- Fluorescence map
- Only spent fuel sample at synchrotron???
- [Np] drops with 20 microns from 1:1500 to 1:7000 proportional U 4+/6+ fraction

Figure 2.2. Miniature Drill Press for Coring CSNF Specimens Using a Hollow Stainless Steel Bit with Diamond Abrasive, Shown in the Hot Cell

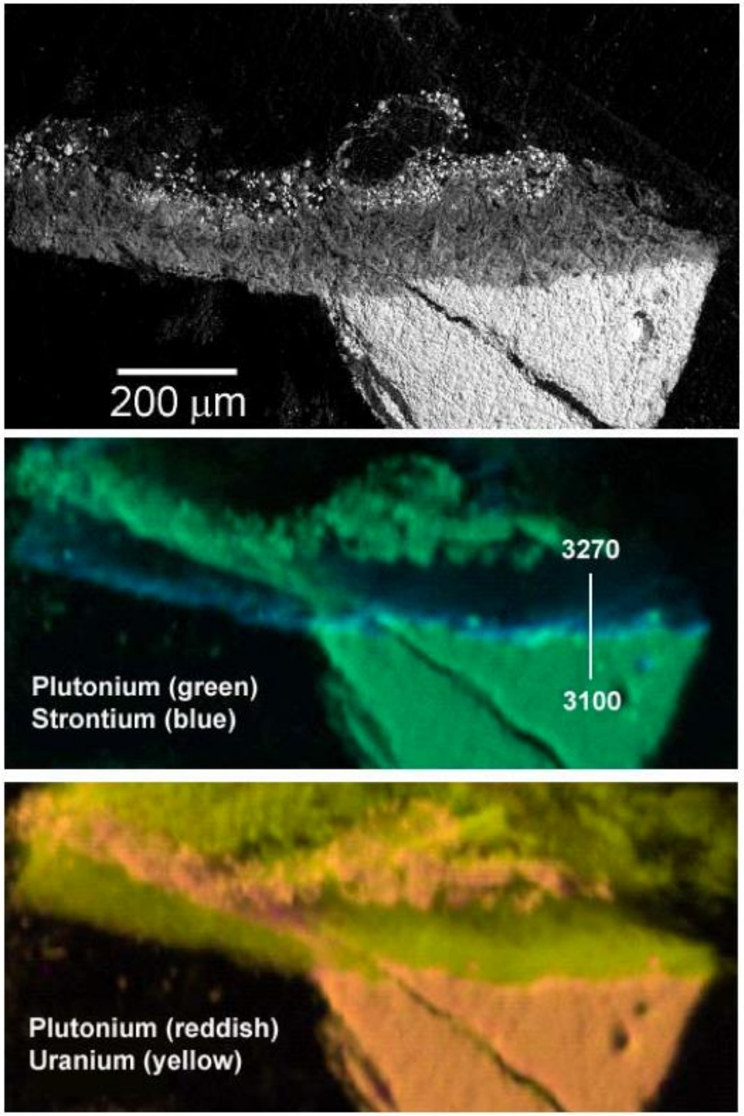

Kropf, Fortner, DOE-OSTI Report www.ipd.anl.gov/anlpubs/2006/11/57766.pdf

Electron Microscopy

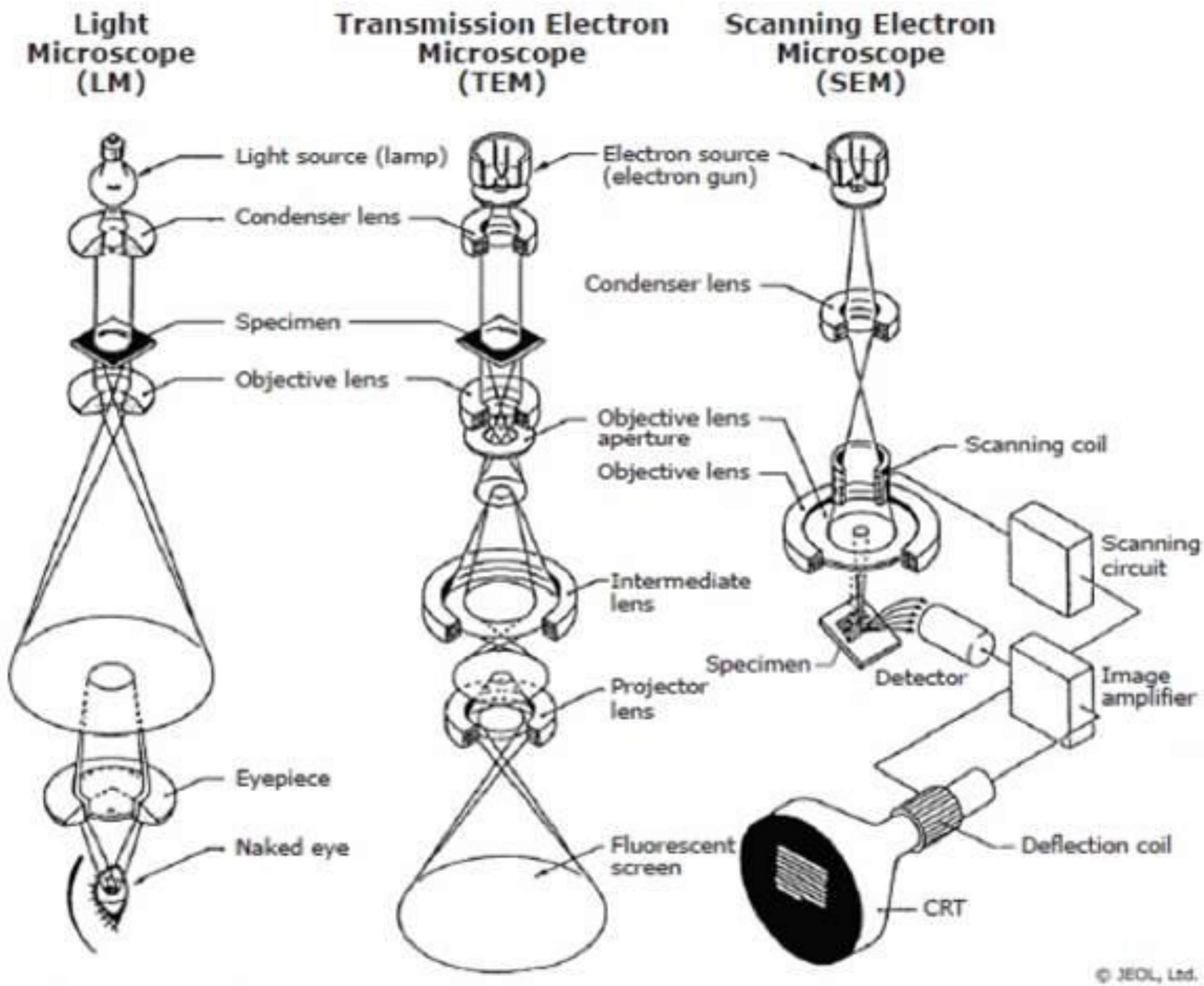

JEOL Manual

Scanning Electron Microscopy (SEM)

- Secondary Electrons
  - Lost energy due to inelastic scattering
  - Sensitive to physical structure (topography)
- Backscattered Electrons
  - Elastically scattered
  - Sensitive to atomic number (elemental)
- X-ray Fluorescence
  - Collisionally excited states relax emitting X-rays

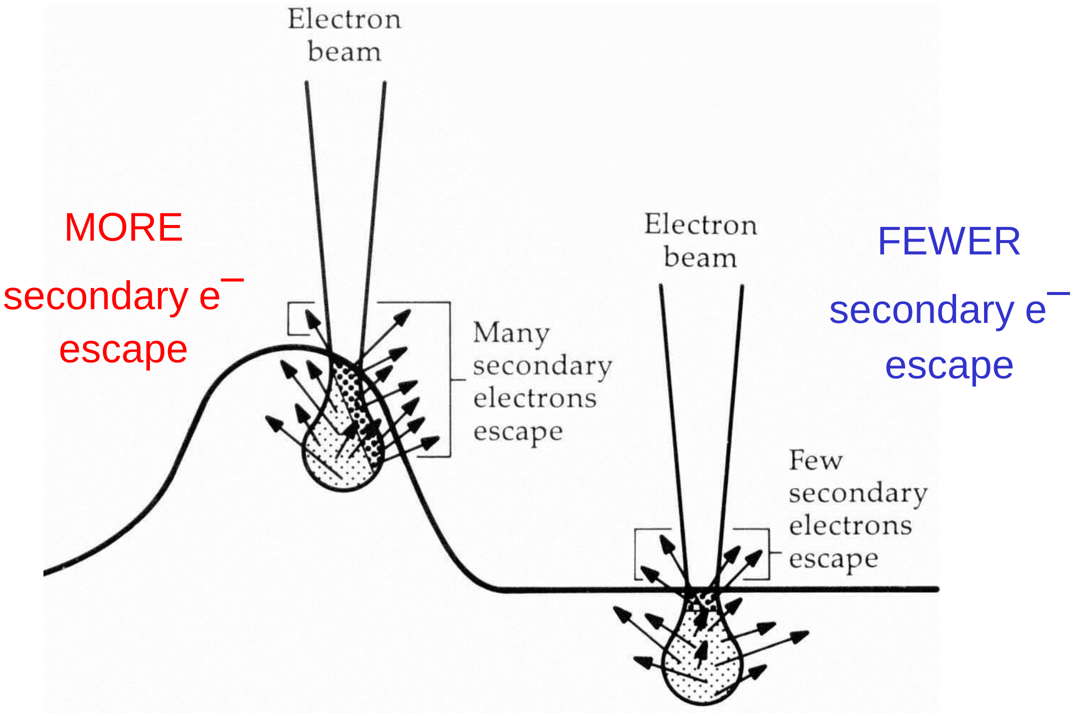

JEOL Manual

SEM Boron Nitride

- Large BN flakes grown on thin film silver

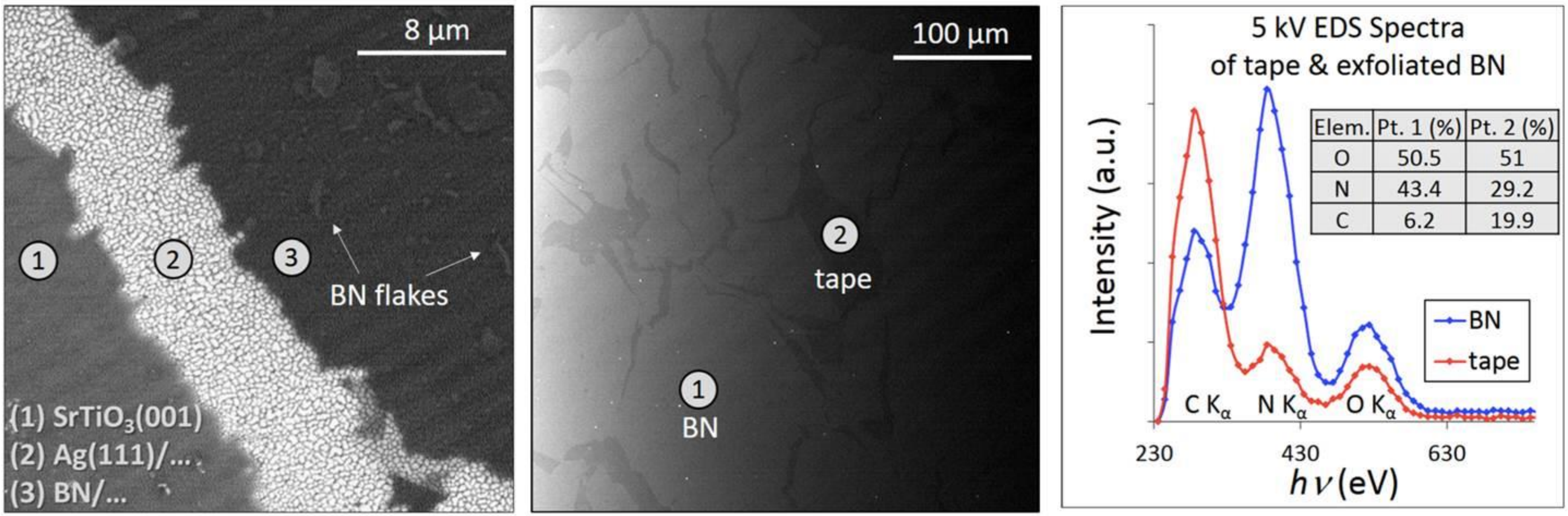

(a) 5 kV image (b) 5 kV image (c) 5 kV spectra

Velazquez, et al., JOURNAL OF APPLIED PHYSICS 119, 095306 (2016)

Transmission Electron Microscopy (TEM)

- Topography
- Morphology
- Composition
- Crystallography

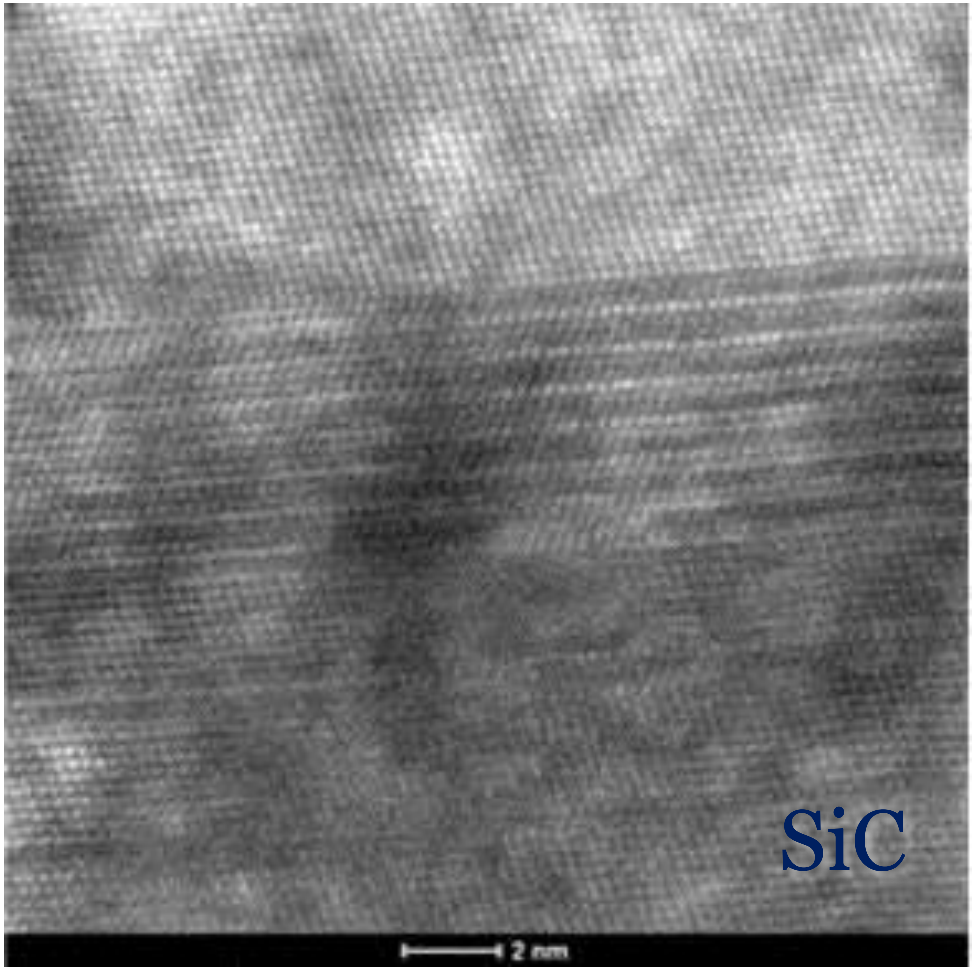

Seibert, et al., in preparation

TEM

- Thin (<100nm) specimen
- Electrons illuminate the specimen
- Objective lenses form an image or a diffraction pattern
- Electrons either pass through the sample unimpeded, or are scattered
- Image is viewed on a fluorescent screen

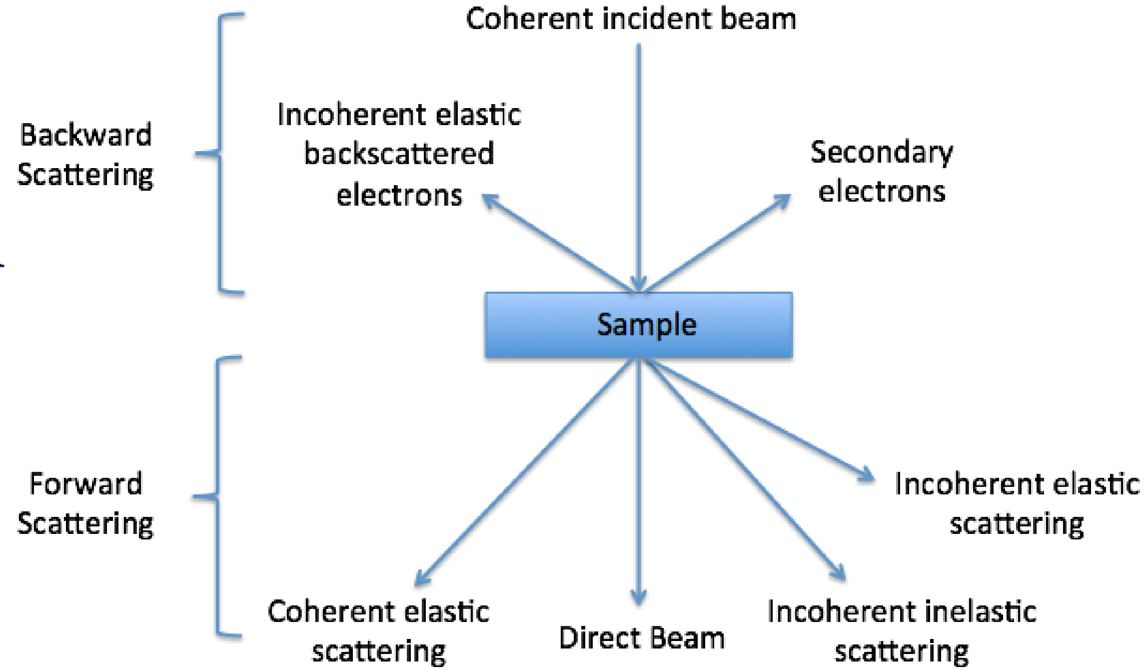

TEM

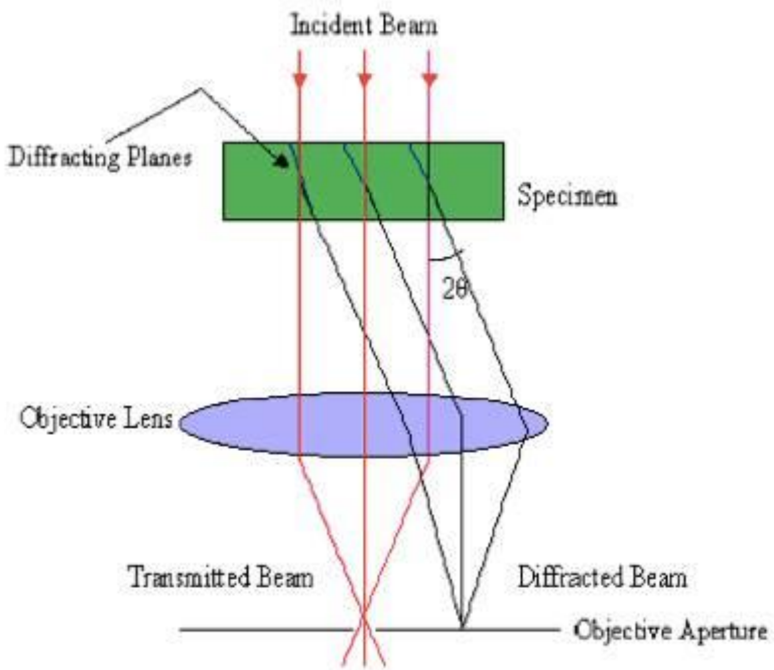

Bright field

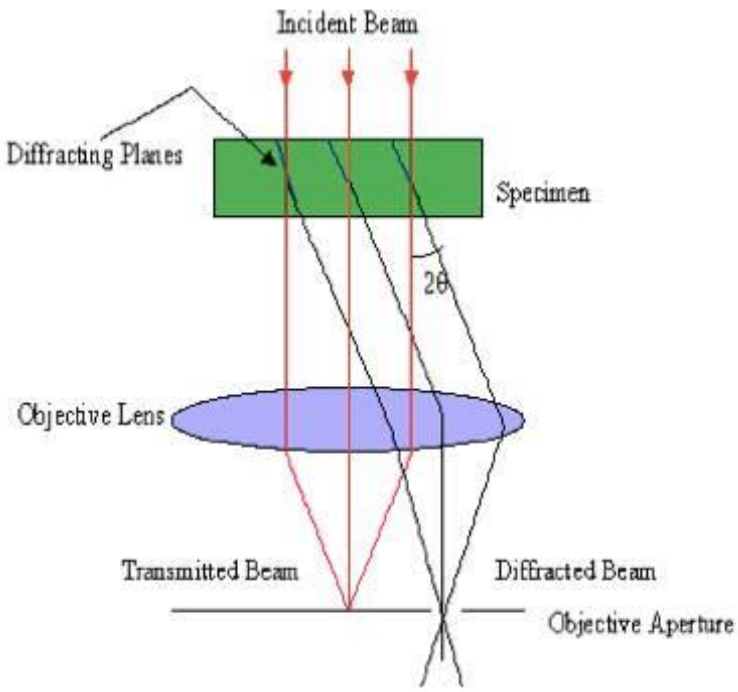

Dark field

Petrova, PhD Dissertation (2006)

High Angle, Annular Dark field (HAADF)

- High scattering angle
- Inelastic, incoherent electrons
- No diffraction

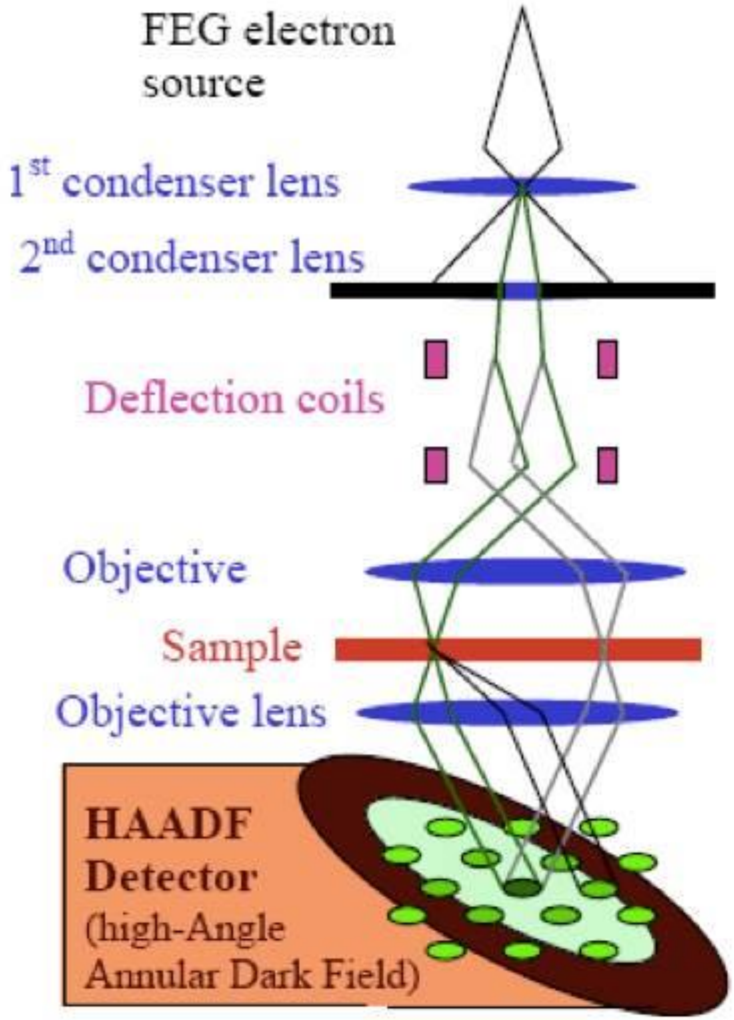

Senapati, MS Dissertation (2005)

TEM ZrC

- Dislocation loops
- TEM - proton irradiated 1.5 DPA @ 800 °C
- White arrows edge-on dislocation loops on (111) planes
- Angle between the edge-on dislocations on different (111) planes is ~70.5°

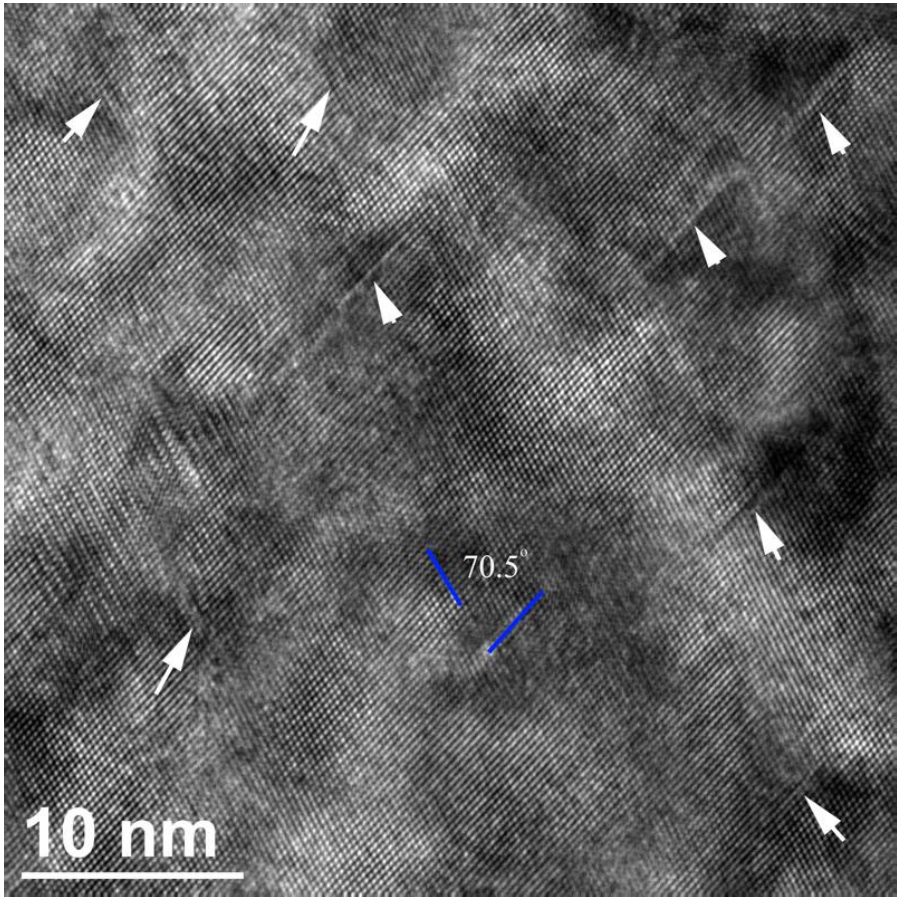

Olive, et al., Journal of Nuclear Materials 475, 123 (2016)

Scanning Probe Microscopy

- Scanning Tunneling Microscopy
  - Tunneling current to tip
- Atomic Force Microscopy
  - Force on tip

SPM

- Tip dragged across a sample

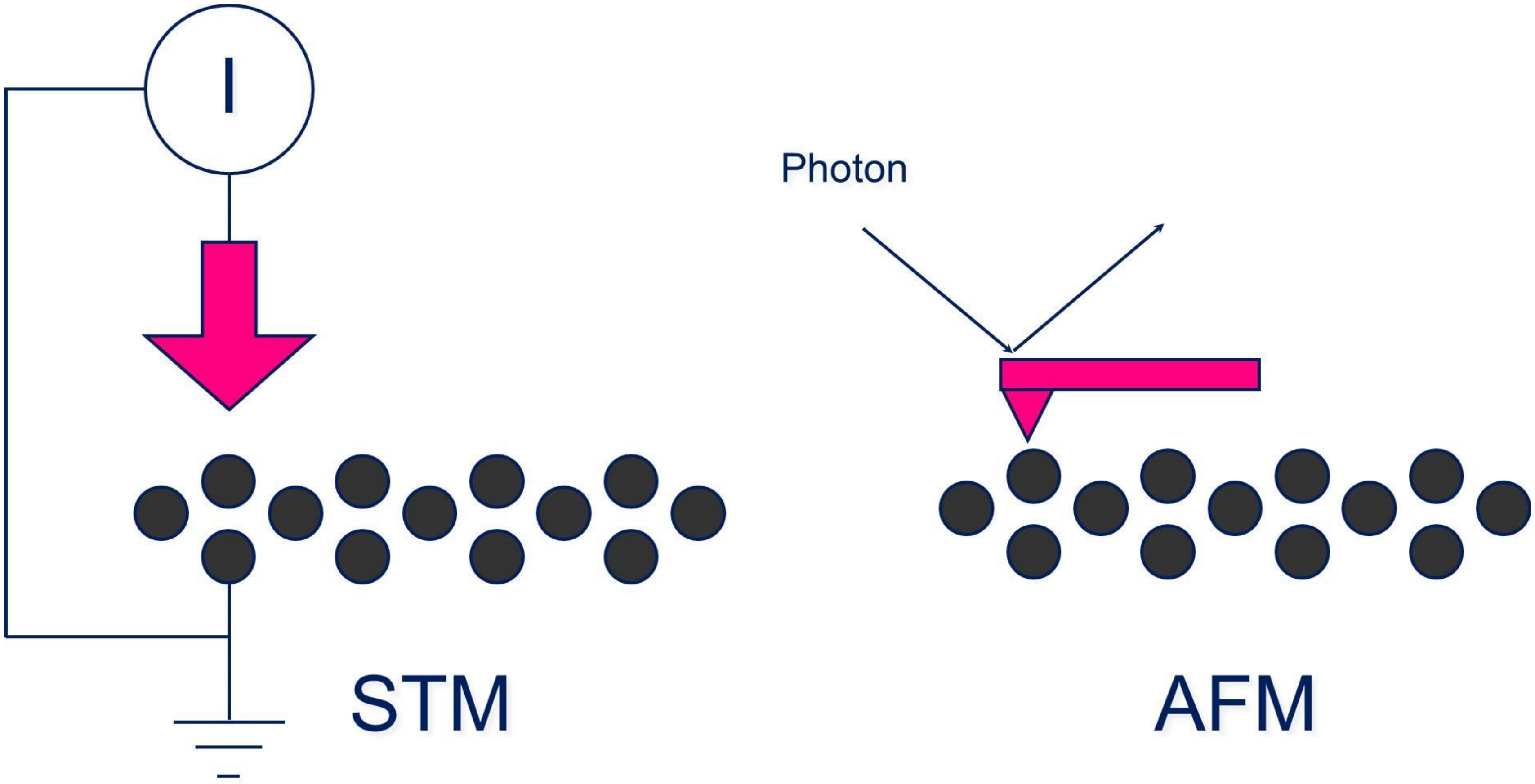

Ag on Si(111)

- Single atomic step islands of epitaxial Ag on Si(111)

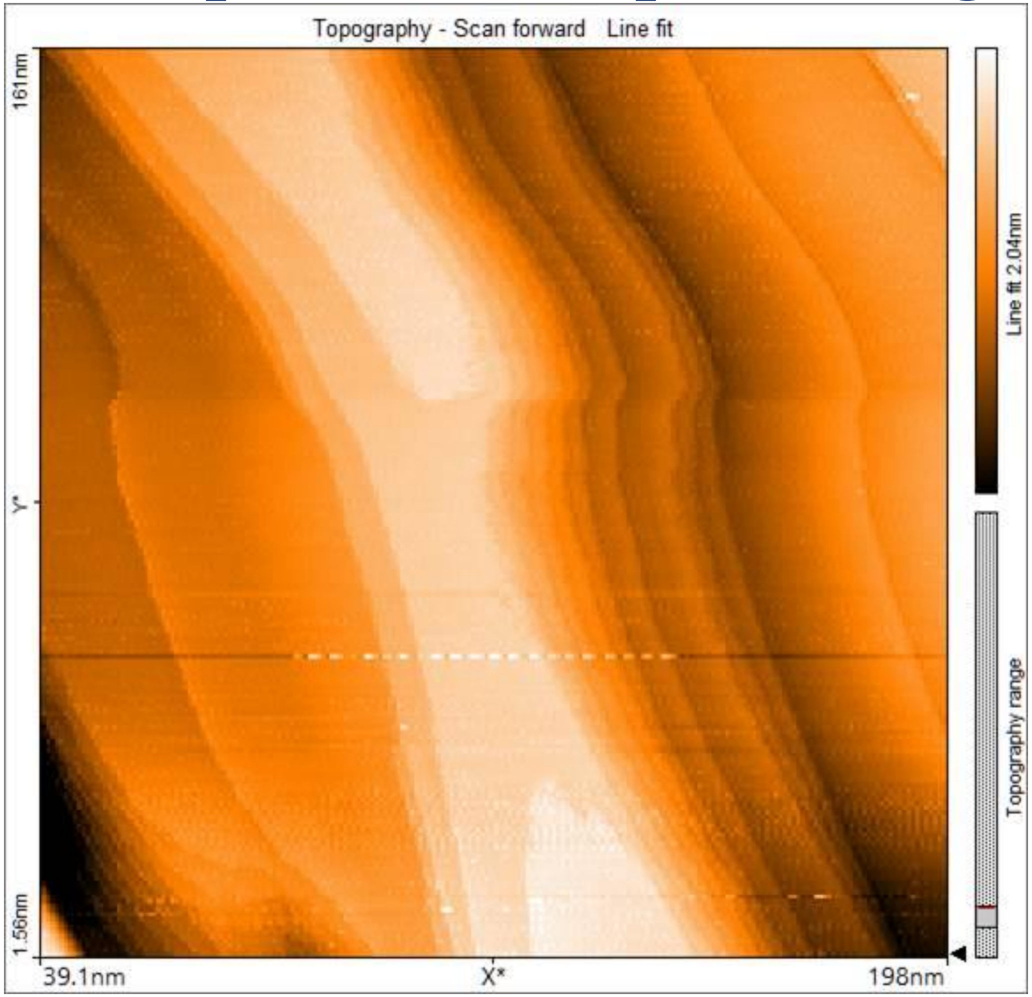

Velazquez, et al., Applied Surface Science 360, 762 (2016)

Putting Them All Together to Tell a Story

- Accident tolerant fuels
- High temperature reactors
  - TRISO Fuel

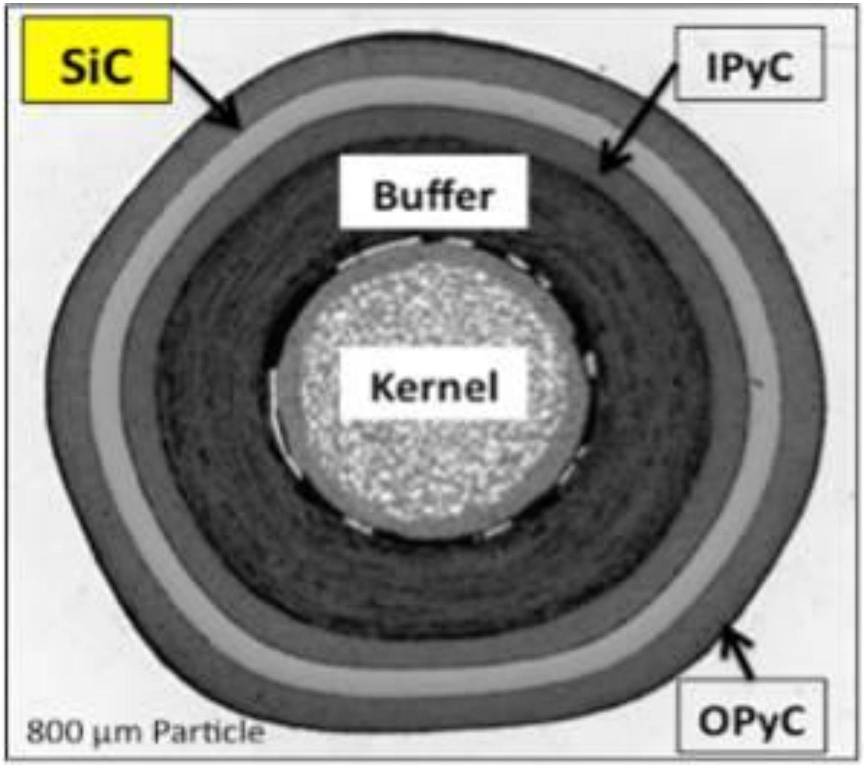

As-fabricated TRISO fuel particle

Seibert, et al., in preparation

Barrier Layer

- SiC is the barrier layer in TRISO fuels
- To get TRISO fuels qualified for use
  - Must understand mechanisms of damage

Irradiated TRISO

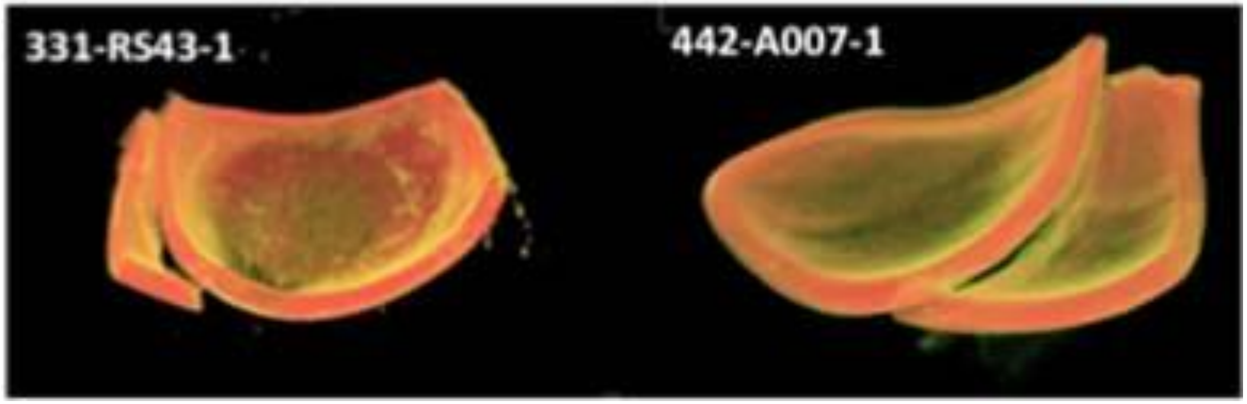

X-ray Tomography of SiC fragments – C. Silva (ORNL)

- Irradiated in the Advanced Test Reactor
- After deconsolidation, select particles annealed to high temperatures for accident simulation
- Isolation of SiC shell through chemical processing

Irradiated TRISO

Parent Particle	Safety Testing	%FIMA	Ag Retention
611-AG59	None	15%	15%
331-RS43	300 hrs 1700 °C	19%	100% post-Test
422-A007	600 hrs 1800 °C	17%	Undetectable post-test

Fluorescence

- Elemental analysis

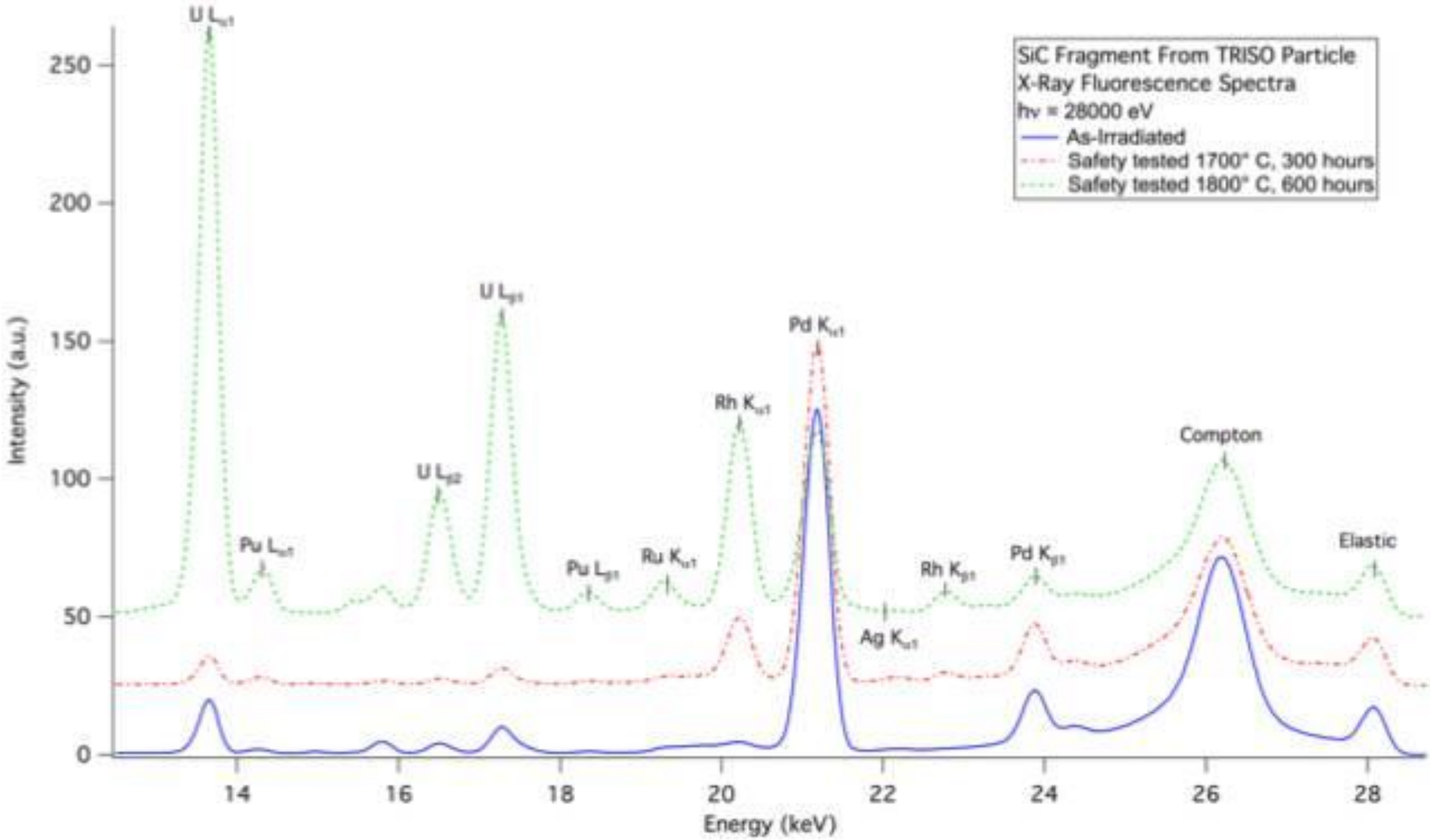

Seibert, et al., in preparation

XAS

- Ag is metallic
  - May be an alloy

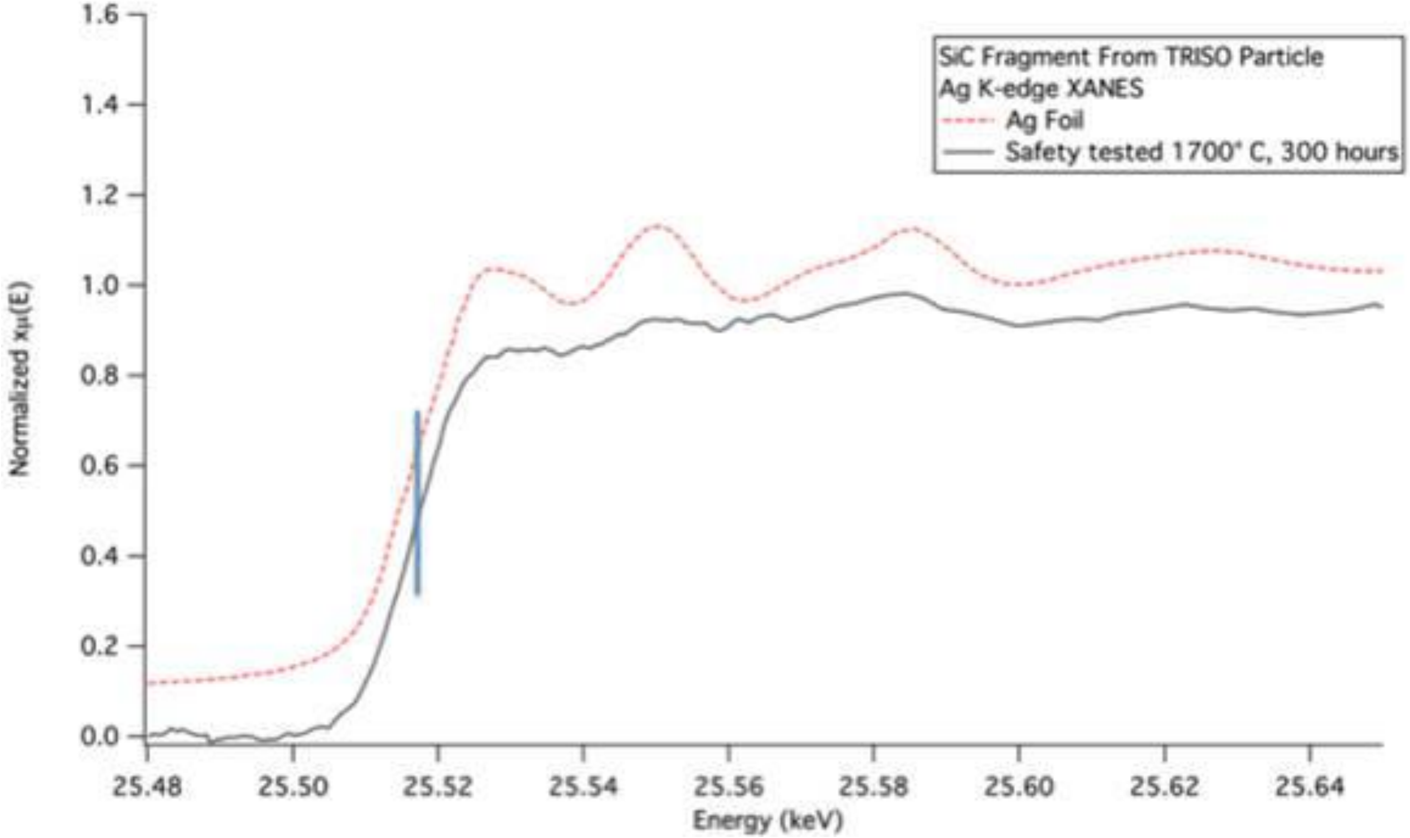

Seibert, et al., in preparation

Microscopy

- Focused Ion Beam Milling

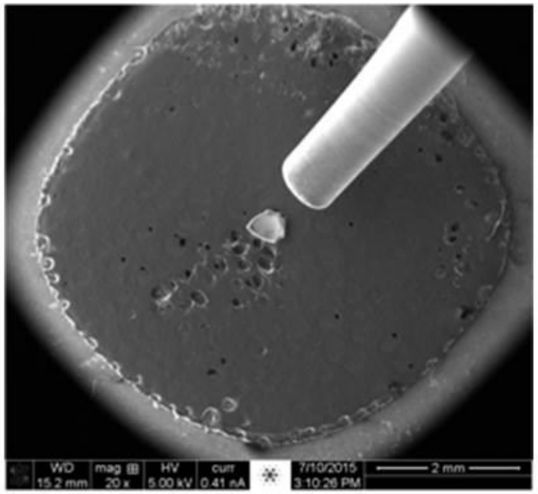

Particle is in the center of a 5mm carbon dot

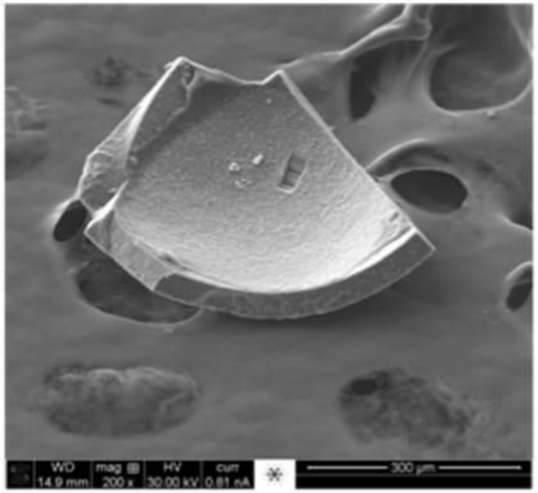

Close-up of the particle curvature that must be worked with during sample preparation

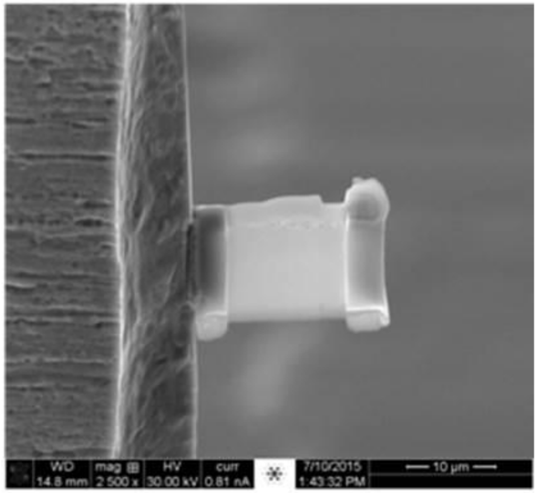

Fully thinned specimen prepared for TEM analysis

Seibert, et al., in preparation

As-Irradiated Sample: IPyC/SiC Interface

- High angle, annular dark field shows high Z

Bright Field HAADF

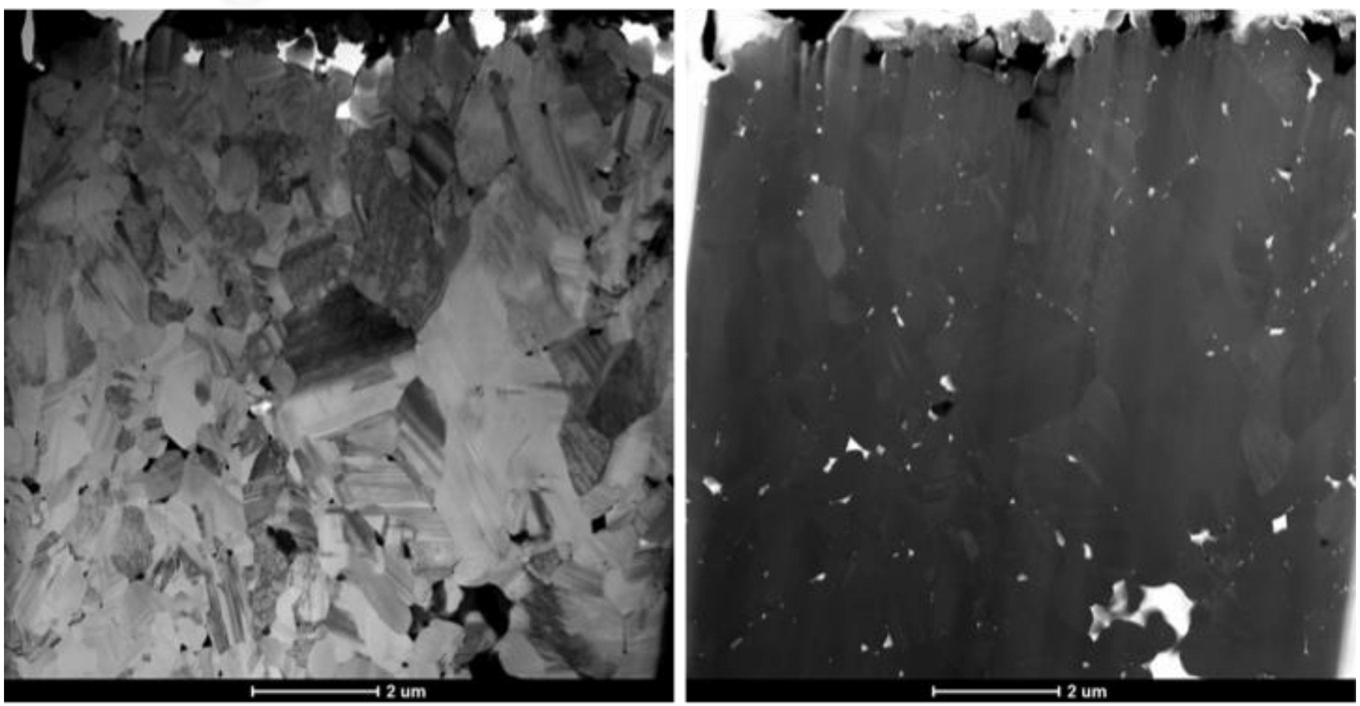

Seibert, et al., in preparation

As-Irradiated Sample: IPyC/SiC Interface

- Lot of overlap among fission products
- Some co-location with actinides

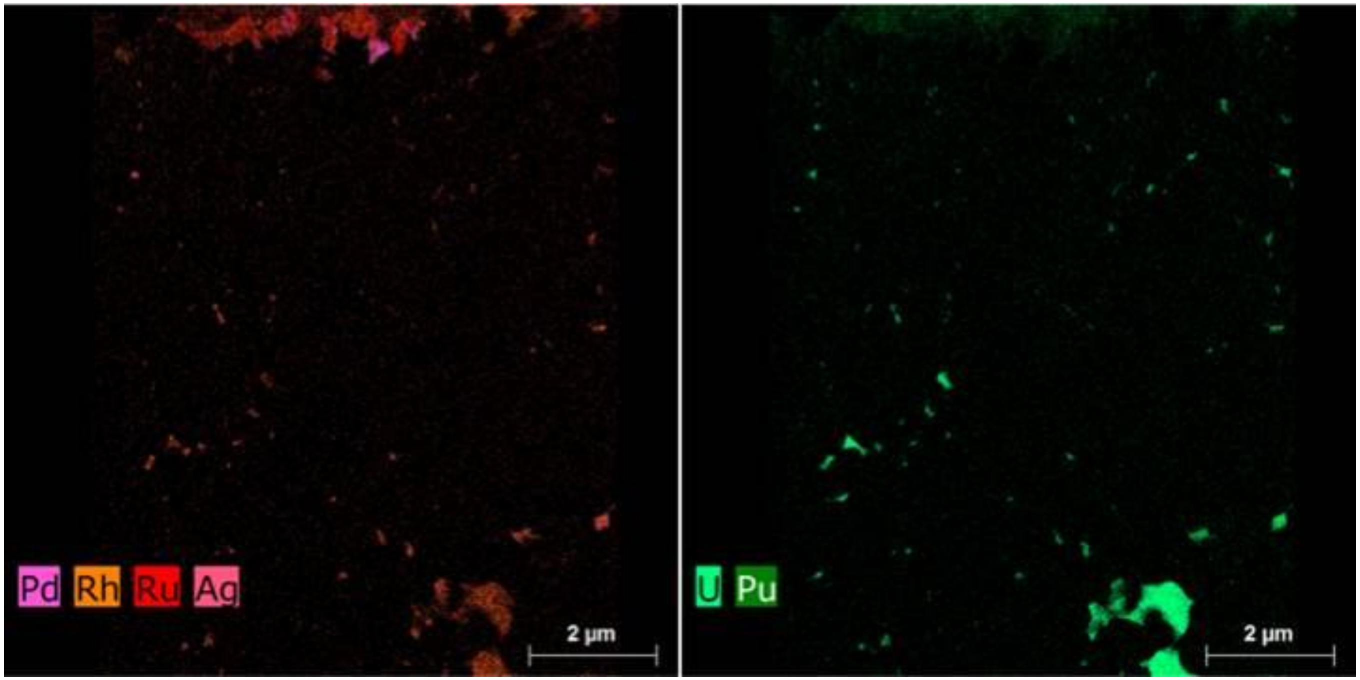

Fission Actinides

Seibert, et al., in preparation

What Did We Learn By Combining Techniques?

- Fission products and actinides found along grain boundaries and triple points in the SiC.
- Fission products (specifically Pd) found all the way to the OPyC interface
- U has been found in large quantities as deep as 13μm from the IPyC interface, and in trace quantities near the OPyC interface
- Ag is metallic

Safety Concerns

- Working with radioactive materials does require extra precaution
- Minimize worker exposure
  - Use long tools
  - Redesign holders to minimize handling time

Safety

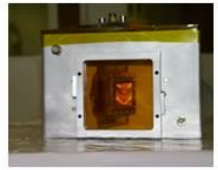

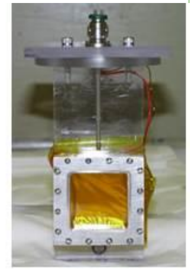

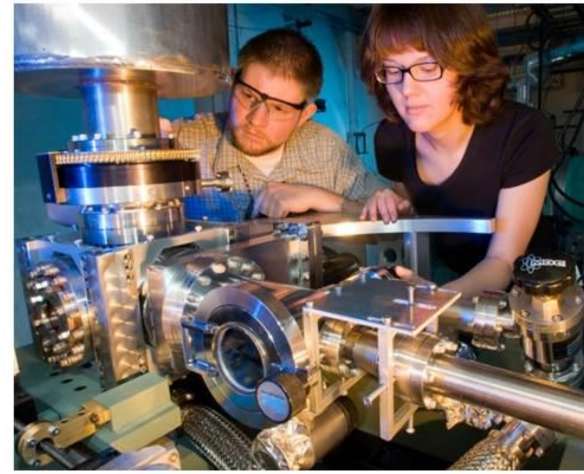

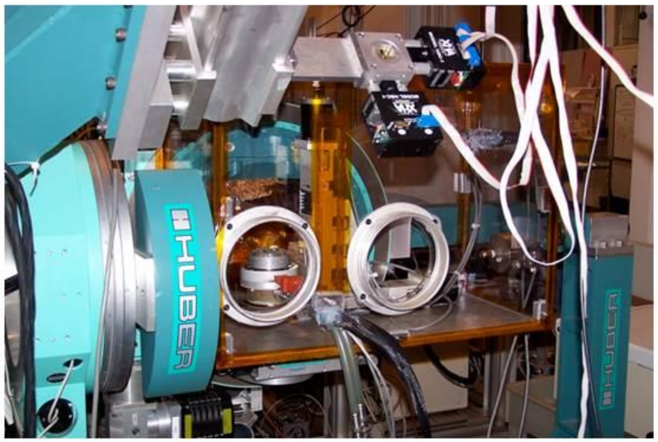

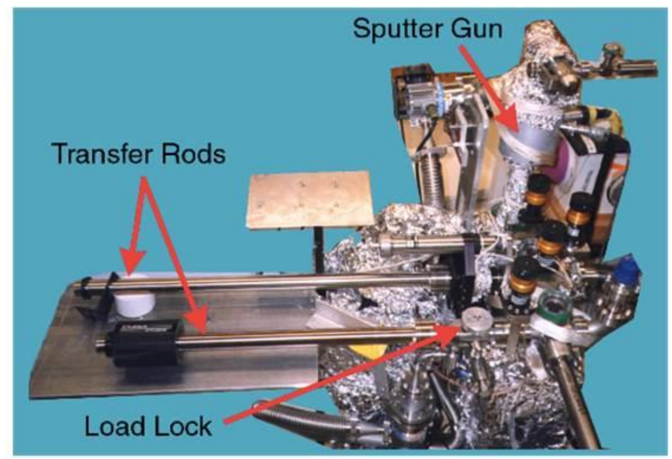

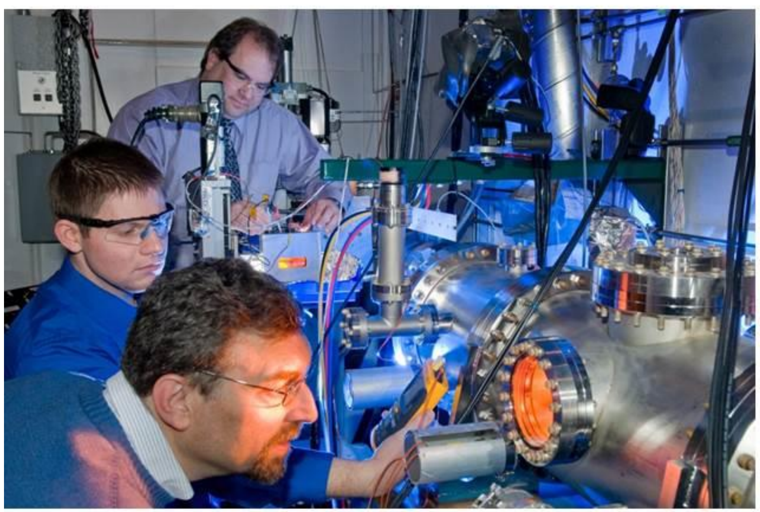

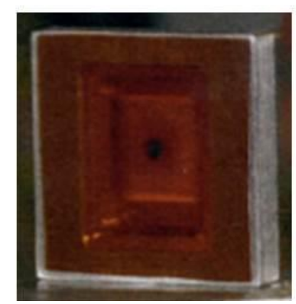

Terry, unpublished

Nuclear Science User Facility

- Almost all of these techniques are available to all through the Nuclear Science User Facility
  - Write a proposal
  - If awarded, assigned Subject Matter Expert to work with you
  - Great way to get access to these techniques

References

- Rotenberg: www-b17.lbl.gov/BL7/who/eli/SRSchoolER.pd
- Terry, J, et al., Surface Science 499, L141 (2002)
- Tobin, J. G, et al., Physical Review B 68, 155109 (2003)
- Cole, et al., J. Phs.:Condens. Matter 10 (1998) 5679-5695
- Martin, et al, Physical Review B 72, 054210 (2005)
- W. Olovsson et al, Journal of Electron Spectroscopy and Related Phenomena 178-179 (2010) 88-99
- J. Stohr Nexafs Spectroscopy
- Kuri, et al., Appl Phys A (2010) 98: 625–633
- Olive, et al., Journal of Nuclear Materials 475, 123 (2016)
- Liu, et al., Materials Science & Engineering A 651, 55 (2016)
- Okuniewski, et al., J. Nuc. Mater., submitted
- Kim, et al., Materials Transactions, Vol. 50, No. 4 (2009) pp. 917 to 921
- Zabler, et al., OPTICS LETTERS 32, 2987 (2007)
- Sun, et al., AIP Conf. Proc. 1430, 1251-1258 (2012)
- Strietelmeier, et al, LBNL/ALS—29523 (1999)
- Kropf, Fortner, DOE-OSTI Report www.ipd.anl.gov/anlpubs/2006/11/57766.pdf
- JEOL Manual
- Velazquez, et al., JOURNAL OF APPLIED PHYSICS 119, 095306 (2016)
- Petrova, PhD Dissertation (2006)
- Senapati, MS Dissertation (2005)
- Velazquez, et al., Applied Surface Science 360, 762 (2016)
- Seibert, et al., in preparation
- C. Silva, ORNL

Students and Postdocs

- Dan Olive
- Hasitha Ganegoda
- Daniel Velazquez
- Joshua Wright
- Hamdi Man
- Rachel Seibert
- ZhengRong Lee

Questions???

Upcoming Webinars

- Nuclear Materials Analysis — Chemical Methods
- Nuclear Materials Analysis — Non-Destructive Analysis
- Nuclear Materials Analysis — Mass Spectoscopy

NAMP website: www.wipp.energy.gov/namp